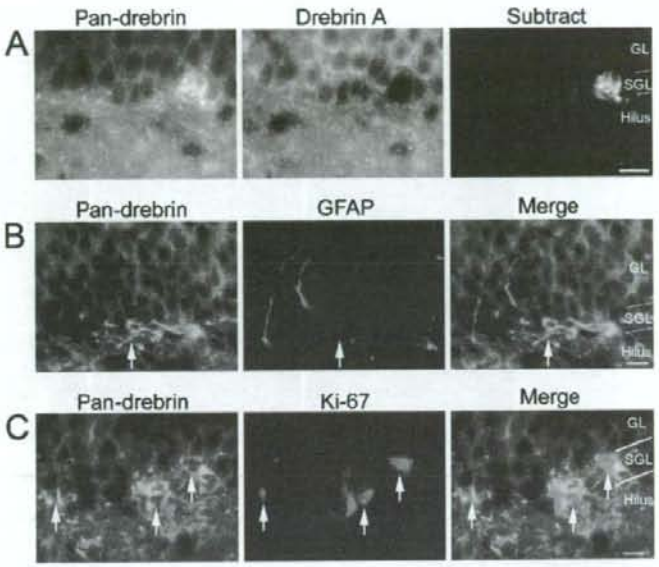

Fig. 10. Characteristics of drebrin distribution in DG. (A) The left and middle panels show images stained with the anti-pan-drebrin (M2F6) and anti-drebrin A (DAS2) antibodies, respectively. The right panels show the subtraction images obtained by subtracting the DAS2 image from the M2F6 image. The subtraction image shows clustered small cells with drebrin E+A− signals in the SGL. (B, C) The left panels show images of cells stained with M2F6 (green), and the middle panels show images of those stained with anti-GFAP (B) and anti-K_i-67 (C) antibodies (red). The right panels show merged images of the left and middle images. Drebrin immunostaining (indicated by arrows in B) does not overlap with GFAP immunostaining. Part of drebrin immunostaining surrounds the cell nuclei stained with the anti-K_i-67 antibody (indicated by arrows in C). GL, granular layer. Scale bars=10 μm.

ing that drebrin A accumulates probably together with drebrin E in dendritic spines but not in cell bodies.

The binding of drebrin to actin filaments is thought to affect the organization of the actin cytoskeleton by the following two mechanisms (Shirao, 1995; Sekino et al., 2007). First, drebrin E suppresses the cross-linking of actin filaments, because drebrin competes with actin-cross-linking proteins, such as α-actinin (Ishikawa et al., 1994) and

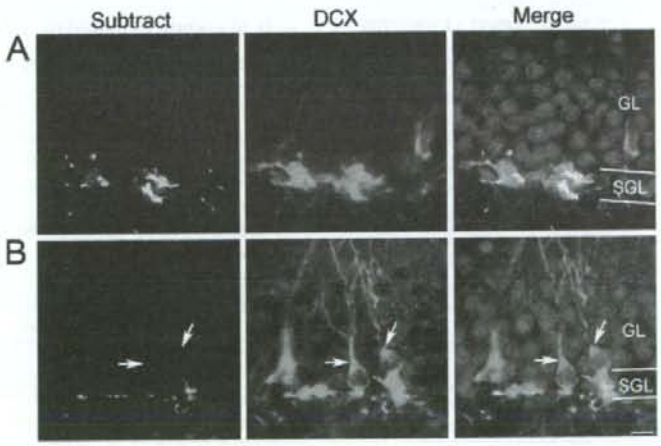

Fig. 11. Comparison of drebrin E+A− and DCX signals in DG. The left panels show subtraction images representing drebrin E+A− signals. The middle panels show images of cells stained with an anti-DCX antibody. The right panels show merged images of drebrin E+A− (green), DCX (red), and DAPI (blue) signals. (A) DCX-immunopositive cells in the SGL are sometimes highlighted by drebrin E+A− signals. Note that cells with drebrin E+A− signals had smaller cell bodies. (B) DCX-immunopositive cells (indicated by arrows in B), which have apical dendrites extending to the outer part of the granular layer (upper direction), are not highlighted by drebrin E+A− signals. GL, granular layer. Scale bar=10 μm.

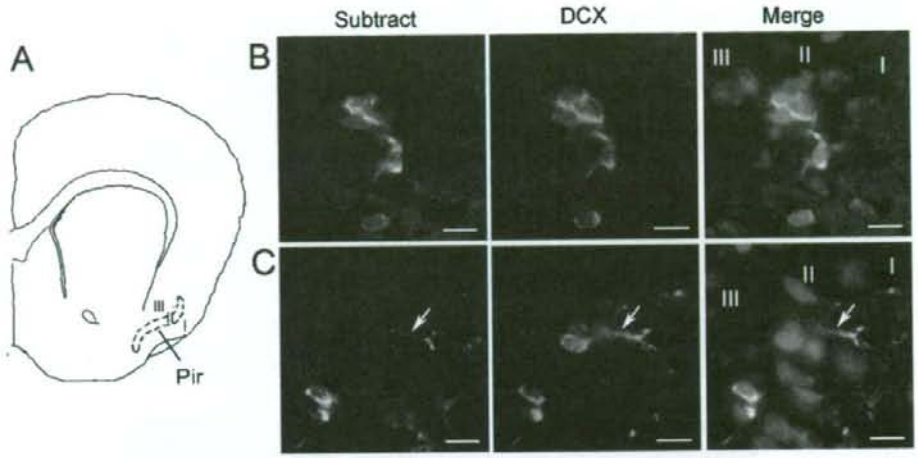

Fig. 12. Cells with drebrin E+A− signals in layer II of adult piriform cortex. (A) Schematic drawing of piriform cortex. (B, C) The left panels show subtraction images representing drebrin E+A− signals. The middle panels show images of cells stained with anti-DCX antibody. The right panels show merged images of drebrin E+A− (green), DCX (red), and DAPI (blue) signals. Note that clustered cells with drebrin E+A− signals were immunostained with the anti-DCX antibody (B). A cell body extending apical dendrites (indicated by arrows) to layer I (right direction) was not highlighted by drebrin E+A− signals (C). Scale bars=10 μm.

fascin (Sasaki et al., 1996), in binding to actin filaments. Second, drebrin E may destabilize actin filaments, because it inhibits the actin-binding activity of tropomyosin, which protects actin filaments from being severed by the action of gelsolin (Ishikawa et al., 1994). Thus, drebrin strongly modifies the structural property of actin filaments and regulates the interactions of actin filaments with many other actin-binding proteins. In this regard, the regulation by this side-binding protein of actin filaments might be upstream of the regulation by other actin-associated proteins. Therefore, the disappearance of drebrin E from the cell body may be involved in the cessation of neuronal migration through the change in the actin cytoskeletal organization in the cell body.

The disappearance of drebrin E+A− signals from cell body and the appearance of drebrin A occur almost simultaneously, suggesting that appearance of drebrin A is involved in the change in drebrin distribution. However, this is unlikely because an *in vitro* study using neuroblastoma cells showed that drebrin can change its distribution without undergoing any isoform change, when the cells differentiate as induced by retinoic acid (Asada et al., 1994).

Because DCX regulates microtubule polymerization and bundling both *in vitro* and *in vivo* (Gleeson et al., 1999; Horesh et al., 1999), it may direct neuronal migration by regulating mainly the organization and stability of microtubules. However, it is also possible that DCX is involved in the neuronal migration through actin cytoskeleton, since it was recently demonstrated that DCX also bind to actin filaments (Tsukada et al., 2005). Previous studies show that DCX is expressed in migrating neuroblasts in the adult brain (Nacher et al., 2001; Brown et al., 2003; Rao and Shetty, 2004; Couillard-Despres et al., 2005). This study also shows that DCX, as well as drebrin E+A− signals, is detected in migrating neurons in both the SVZ–RMS–OB system and the hippocampal DG. However, in contrast to drebrin E+A− signals, DCX is continuously detected for sometime after the cessation of migration; moreover, DCX is distributed in whole cell bodies and branching dendrites of young neurons, which is consistent with the finding of a previous study (Francis et al., 1999). These observations suggest that the change in the regulation of the microtubule cytoskeletal organization is not specifically involved in the cessation of adult neuronal migration.

Role of drebrin in migrating neuroblasts

This study shows that migrating neuroblasts express only drebrin E, although drebrin A is the predominant isoform in the adult brain. This suggests that the migratory mechanism of neuroblasts is similar to that of non-neuronal cells at least in terms of the actin cytoskeleton, because drebrin E is the isoform expressed in both non-neuronal cells and neurons.

Many previous observations derived mostly from the study of drebrin E suggest the association of drebrin with cell migration. Drebrin seems to be involved in the cell polarization, which is the first step in cell migration, because it shows distinct localization in polarized cells, such as acid-secreting cells of the gastric gland and kidney (Keon et al., 2000). Furthermore, drebrin forms actin-anchoring junctional plaques distinct from vinculin-based plaques (Peitsch et al., 1999) and regulates cell-substrate adhesion (Ikeda et al., 1995, 1996). It also inhibits actomyosin interaction and reduces the sliding velocity of actin filaments on myosin (Hayashi et al., 1996). Recently, drebrin has been reported to contribute to the retraction of the cell bodies and tails of migrating melanoma cells (Peitsch

et al., 2006). Taken together, these findings indicate that drebrin E plays a role in cell migration by modifying the organization of actin cytoskeletons and cell-substrate adhesion, and by regulating the contractile force required to move the cell body forward.

CONCLUSION

In conclusion, drebrin E but not drebrin A is detected in the cell body of migrating neuroblasts in the adult brain. The disappearance of drebrin E from the cell body coincides with the cessation of migration. Because drebrin modifies the characteristics of actin filaments, the disappearance of drebrin E from the cell body causes a change in the organization of the actin cytoskeleton, suggesting that the actin cytoskeleton plays a pivotal role in the cessation of adult neuronal migration. Furthermore, our results suggest that drebrin is a molecular switch for neuronal migration. Because the regulatory mechanism of neuronal migration is important for the appropriate targeting and integration of newly generated neurons into existing neuronal networks, in a future study, it will be of interest to identify extrinsic signals that change the distribution of drebrin E in migrating neuroblasts.

Acknowledgments—This work was supported in part by Grants-in-Aid for Scientific Research on Priority Areas-Elucidation of neural network function in the brain from the Ministry of Education, Culture, Sports, Science and Technology of Japan (MEXT) (17023008). We thank Drs. Kunihiko Obata, Kenichi Uyemura and Hideto Takahashi for helpful comments. We also thank Dr. Pokay Ma for editing this manuscript.

REFERENCES

Aoki C, Sekino Y, Hanamura K, Fujisawa S, Mahadomrongkul V, Ren Y, Shirao T (2005) Drebrin A is a postsynaptic protein that localizes in vivo to the submembranous surface of dendritic sites forming excitatory synapses. J Comp Neurol 483:383–402.

Asada H, Uyemura K, Shirao T (1994) Actin-binding protein, drebrin, accumulates in submembranous regions in parallel with neuronal differentiation. J Neurosci Res 38:149–159.

Bai J, Ramos RL, Ackman JB, Thomas AM, Lee RV, LoTurco JJ (2003) RNAi reveals doublecortin is required for radial migration in rat neocortex. Nat Neurosci 6:1277–1283.

Brown JP, Couillard-Despres S, Cooper-Kuhn CM, Winkler J, Aigner L, Kuhn HG (2003) Transient expression of doublecortin during adult neurogenesis. J Comp Neurol 467:1–10.

Butkevich E, Hulsmann S, Wenzel D, Shirao T, Duden R, Majoul I (2004) Drebrin is a novel connexin-43 binding partner that links gap junctions to the submembrane cytoskeleton. Curr Biol 14:650–658.

Corbo JC, Deuel TA, Long JM, LaPorte P, Tsai E, Wynshaw-Boris A, Walsh CA (2002) Doublecortin is required in mice for lamination of the hippocampus but not the neocortex. J Neurosci 22:7548–7557.

Couillard-Despres S, Winner B, Schaubeck S, Aigner R, Vroemen M, Weidner N, Bogdahn U, Winkler J, Kuhn HG, Aigner L (2005) Doublecortin expression levels in adult brain reflect neurogenesis. Eur J Neurosci 21:1–14.

Deuel TA, Liu JS, Corbo JC, Yoo SY, Rorke-Adams LB, Walsh CA (2006) Genetic interactions between doublecortin and doublecortin-like kinase in neuronal migration and axon outgrowth. Neuron 49:41–53.

Doetsch F, Alvarez-Buylla A (1996) Network of tangential pathways for neuronal migration in adult mammalian brain. Proc Natl Acad Sci U S A 93:14895–14900.

Doetsch F, Garcia-Verdugo JM, Alvarez-Buylla A (1997) Cellular composition and three-dimensional organization of the subventricular germinal zone in the adult mammalian brain. J Neurosci 17: 5046–5061.

Doetsch F, Caille I, Lim DA, Garcia-Verdugo JM, Alvarez-Buylla A (1999) Subventricular zone astrocytes are neural stem cells in the adult mammalian brain. Cell 97:703–716.

Fox JW, Lamperti ED, Eksioglu YZ, Hong SE, Feng Y, Graham DA, Scheffer IE, Dobyns WB, Hirsch BA, Radtke RA, Berkovic SF, Huttenlocher PR, Walsh CA (1998) Mutations in filamin 1 prevent migration of cerebral cortical neurons in human periventricular heterotopia. Neuron 21:1315–1325.

Francis F, Koulakoff A, Boucher D, Chafey P, Schaar B, Vinet MC, Friocourt G, McDonnell N, Reiner O, Kahn A, McConnell SK, Berwald-Netter Y, Denoulet P, Chelly J (1999) Doublecortin is a developmentally regulated, microtubule-associated protein expressed in migrating and differentiating neurons. Neuron 23: 247–256.

Garcia-Verdugo JM, Doetsch F, Wichterle H, Lim DA, Alvarez-Buylla A (1998) Architecture and cell types of the adult subventricular zone: in search of the stem cells. J Neurobiol 36:234–248.

Gleeson JG, Lin PT, Flanagan LA, Walsh CA (1999) Doublecortin is a microtubule-associated protein and is expressed widely by migrating neurons. Neuron 23:257–271.

Gleeson JG, Walsh CA (2000) Neuronal migration disorders: from genetic diseases to developmental mechanisms. Trends Neurosci 23:352–359.

Hayashi K, Ishikawa R, Ye LH, He XL, Takata K, Kohama K, Shirao T (1996) Modulatory role of drebrin on the cytoskeleton within dendritic spines in the rat cerebral cortex. J Neurosci 16:7161–7170.

Horesh D, Sapir T, Francis F, Wolf SG, Caspi M, Elbaum M, Chelly J, Reiner O (1999) Doublecortin, a stabilizer of microtubules. Hum Mol Genet 8:1599–1610.

Ikeda K, Shirao T, Toda M, Asada H, Toya S, Uyemura K (1995) Effect of neuron-specific actin-binding protein, drebrin A, on cell-substratum adhesion. Neurosci Lett 194:197–200.

Ikeda K, Kaub PA, Asada H, Uyemura K, Toya S, Shirao T (1996) Stabilization of adhesion plaques by the expression of drebrin A in fibroblasts. Dev Brain Res 91:227–236.

Ishikawa R, Hayashi K, Shirao T, Xue Y, Takagi T, Sasaki Y, Kohama K (1994) Drebrin, a development-associated brain protein from rat embryo, causes the dissociation of tropomyosin from actin filaments. J Biol Chem 269:29928–29933.

Kee N, Sivalingam S, Boonstra R, Wojtowicz JM (2002) The utility of Ki-67 and BrdU as proliferative markers of adult neurogenesis. J Neurosci Methods 115:97–105.

Keon BH, Jedrzejewski PT, Paul DL, Goodenough DA (2000) Isoform specific expression of the neuronal F-actin binding protein, drebrin, in specialized cells of stomach and kidney epithelia. J Cell Sci 113:325–336.

Kirschenbaum B, Doetsch F, Lois C, Alvarez-Buylla A (1999) Adult subventricular zone neuronal precursors continue to proliferate and migrate in the absence of the olfactory bulb. J Neurosci 19:2171–2180.

Kojima N, Shirao T, Obata K (1993) Molecular cloning of a developmentally regulated brain protein, chicken drebrin A and its expression by alternative splicing of the drebrin gene. Mol Brain Res 19:101–114.

Koizumi H, Higginbotham H, Poon T, Tanaka T, Brinkman BC, Gleeson JG (2006) Doublecortin maintains bipolar shape and nuclear translocation during migration in the adult forebrain. Nat Neurosci 9:779–786.

Lambert de Rouvroit C, Goffinet AM (2001) Neuronal migration. Mech Dev 105:47–56.

Lois C, Alvarez-Buylla A (1994) Long-distance neuronal migration in the adult mammalian brain. Science 264:1145–1148.

Lois C, Garcia-Verdugo JM, Alvarez-Buylla A (1996) Chain migration of neuronal precursors. Science 271:978–981.

Nacher J, Crespo C, McEwen BS (2001) Doublecortin expression in the adult rat telencephalon. Eur J Neurosci 14:629–644.

Paxinos G, Watson C (1998) The rat brain in stereotaxic coordinates, 4th ed. San Diego, CA: Academic Press.

Peitsch WK, Grund C, Kuhn C, Schnolzer M, Spring H, Schmelz M, Franke WW (1999) Drebrin is a widespread actin-associating protein enriched at junctional plaques, defining a specific microfilament anchorage system in polar epithelial cells. Eur J Cell Biol 78:767–778.

Peitsch WK, Bulkescher J, Spring H, Hofmann I, Goerdt S, Franke WW (2006) Dynamics of the actin-binding protein drebrin in motile cells and definition of a juxtanuclear drebrin-enriched zone. Exp Cell Res 312:2605–2618.

Peretto P, Merighi A, Fasolo A, Bonfanti L (1997) Glial tubes in the rostral migratory stream of the adult rat. Brain Res Bull 42:9–21.

Peretto P, Merighi A, Fasolo A, Bonfanti L (1999) The subependymal layer in rodents: a site of structural plasticity and cell migration in the adult mammalian brain. Brain Res Bull 49:221–243.

Rao MS, Shetty AK (2004) Efficacy of doublecortin as a marker to analyse the absolute number and dendritic growth of newly generated neurons in the adult dentate gyrus. Eur J Neurosci 19:234–246.

Rousselot P, Lois C, Alvarez-Buylla A (1995) Embryonic (PSA) N-CAM reveals chains of migrating neuroblasts between the lateral ventricle and the olfactory bulb of adult mice. J Comp Neurol 351:51–61.

Sasaki Y, Hayashi K, Shirao T, Ishikawa R, Kohama K (1996) Inhibition by drebrin of the actin-bundling activity of brain fascin, a protein localized in filopodia of growth cones. J Neurochem 66:980–988.

Scholzen T, Gerdes J (2000) The Ki-67 protein: from the known and the unknown. J Cell Physiol 182:311–322.

Seki T, Arai Y (1991) Expression of highly polysialylated NCAM in the neocortex and piriform cortex of the developing and the adult rat. Anat Embryol 184:395–401.

Sekino Y, Kojima N, Shirao T (2007) Role of actin cytoskeleton in dendritic spine morphogenesis. Neurochem Int 51:92–104.

Shirao T, Obata K (1985) Two acidic proteins associated with brain development in chick embryo. J Neurochem 44:1210–1216.

Shirao T, Obata K (1986) Immunochemical homology of 3 developmentally regulated brain proteins and their developmental change in neuronal distribution. Dev Brain Res 29:233–244.

Shirao T, Inoue HK, Kano Y, Obata K (1987) Localization of a developmentally regulated neuron-specific protein S54 in dendrites as revealed by immunoelectron microscopy. Brain Res 413:374–378.

Shirao T, Kojima N, Nabeta Y, Obata K (1989) Two forms of drebrins, developmentally regulated brain proteins, in rat. Proc Jpn Acad Ser B Phys Biol Sci 65:169–172.

Shirao T, Kojima N, Terada S, Obata K (1990) Expression of three drebrin isoforms in the developing nervous system. Neurosci Res Suppl 13:S106–S111.

Shirao T, Taguchi C, Kobayashi S, Uyemura K (1993) Immunohistochemical analysis of rostral migratory stream of neurons in the subependymal layers of postnatal rat. Soc Neurosci Abstr 19:872.

Shirao T, Hayashi K, Ishikawa R, Isa K, Asada H, Ikeda K, Uyemura K (1994) Formation of thick, curving bundles of actin by drebrin A expressed in fibroblasts. Exp Cell Res 215:145–153.

Shirao T (1995) The roles of microfilament-associated proteins, drebrins, in brain morphogenesis: a review. J Biochem 117:231–236.

Takahashi H, Sekino Y, Tanaka S, Mizui T, Kishi S, Shirao T (2003) Drebrin-dependent actin clustering in dendritic filopodia governs synaptic targeting of postsynaptic density-95 and dendritic spine morphogenesis. J Neurosci 23:6586–6595.

Takahashi H, Mizui T, Shirao T (2006) Down-regulation of drebrin A expression suppresses synaptic targeting of NMDA receptors in developing hippocampal neurones. J Neurochem 97(Suppl. 1): 110–115.

Tsukada M, Prokscha A, Ungewickell E, Eichele G (2005) Doublecortin association with actin filaments is regulated by neurabin II. J Biol Chem 280:11361–11368.

Zhang W, Han S, McKell D, Goate A, Wu J (1998) Interaction of presenilins with the filamin family of actin-binding proteins. J Neurosci 18:914–922.

APPENDIX

Supplementary data

Supplementary data associated with this article can be found, in the online version, at doi: 10.1016/j.neuroscience.2007.10.068.

(Accepted 1 February 2008)
(Available online 19 January 2008)

Cerebral Cortex February 2008;18:315–330
doi:10.1093/cercor/bhm056
Advance Access publication May 20, 2007

Quantitative Chemical Composition of Cortical GABAergic Neurons Revealed in Transgenic Venus-Expressing Rats

Masakazu Uematsu[1,2,3], Yasuharu Hirai[4,5], Fuyuki Karube[4], Satoe Ebihara[1], Megumi Kato[6], Kuniya Abe[7], Kunihiko Obata[1,8], Sachiko Yoshida[2], Masumi Hirabayashi[5,6], Yuchio Yanagawa[1,3,9] and Yasuo Kawaguchi[4,5]

[1]Laboratory of Neurochemistry, National Institute for Physiological Sciences (NIPS), Okazaki 444-8585, Japan, [2]Department of Materials Science, Toyohashi University of Technology, Toyohashi 441-8580, Japan, [3]SORST, JST, Kawaguchi 332-0012, Japan, [4]Division of Cerebral Circuitry, NIPS, [5]Department of Physiological Sciences, The Graduate University for Advanced Studies (SOKENDAI), Okazaki 444-8585, Japan, [6]Center for Genetic Analysis of Behavior, NIPS, [7]BioResource Center, RIKEN Tsukuba Institute, Tsukuba 305-0074, Japan, [8]Neuronal Circuit Mechanisms Research Group, BSI, RIKEN, Wako 351-0198, Japan and [9]Department of Genetic and Behavioral Neuroscience, Gunma University Graduate School of Medicine, Maebashi 371-8511, Japan

The first 2 authors contributed equally to this work.

Although neocortical GABAergic (γ-aminobutyric acidergic) interneurons have been the focus of intense study, especially in the rat, a consensus view of the functional diversity and organization of inhibitory cortical neurons has not yet been achieved. To better analyze GABAergic neurons in the rat, we used a bacterial artificial chromosome (BAC) construct and established 2 lines of transgenic rats that coexpress Venus, a yellow fluorescent protein, with the vesicular GABA transporter. The brain GABA content from both transgenic lines was similar to the level found in wild-type rats. In the frontal cortex, Venus was expressed in >95% of GABAergic neurons, most of which also expressed at least one of 6 biochemical markers, including α-actitin-2, which preferentially labeled late-spiking neurogliaform cells. Taking advantage of the fact that Venus expression allows for targeted recording from all classes of nonpyramidal cells, irrespective of their somatic morphologies, we demonstrated that fast-spiking neurons, which were heterogeneous in somatic size as well as vertical dendritic projection, had relatively uniform horizontal dimensions, suggesting a cell type–specific columnar input territory. Our data demonstrate the benefits of VGAT-Venus rats for investigating GABAergic circuits, as well as the feasibility of using BAC technology in rats to label subsets of specific, genetically defined neurons.

Keywords: bacterial artificial chromosome, cortex, interneuron, transgenic rat, Venus, vesicular GABA transporter

Introduction

Inhibitory neurons in the central nervous system (CNS) are diverse in their morphological and physiological characteristics (Somogyi et al. 1998). To explore the functional diversity of cortical interneurons in the rat neocortex, numerous studies have investigated various aspects of these neurons, such as their axonal and dendritic morphologies, chemical expression patterns, firing patterns, and synaptic connectivity (Kawaguchi and Kubota 1997; Gupta et al. 2000; Kawaguchi and Kondo 2002; Markram et al. 2004; Somogyi and Klausberger 2005; Kubota et al. 2007). However, the implications of the data have been hotly debated, and a consensus view on how these neurons can best be functionally classified has not yet been achieved (Nelson 2002; Yuste 2005). Because the expression of several peptides and calcium-binding proteins is correlated with their physiological and morphological characteristics (Kawaguchi and Kubota 1993; Cauli et al. 2000; Wang et al. 2002; Toledo-Rodriguez et al. 2004; Sugino et al. 2006), as well as their differential response to neuromodulators such as acetylcholine and serotonin (Kawaguchi 1997; Porter et al. 1999; Ferezou et al. 2002; Gulledge et al. 2007), their expression can be used to identify functional subclasses of cortical interneurons. However, it has not yet been determined if these chemical markers identify the entire GABAergic cell population in the neocortex. On the other hand, traditional methods of examining nonpyramidal neurons via intracellular recording may sometimes fail to identify GABAergic (γ-aminobutyric acidergic) cell subtypes that are morphologically and/or physiologically similar to pyramidal neurons. Therefore, selective fluorescent labeling of the entire GABAergic cell population in the rat neocortex would greatly advance the analysis of their cellular and circuit organizations.

To date, transgenic labeling of inhibitory cells in mice has utilized green fluorescent protein (GFP) controlled by the promoter of the biosynthetic enzyme for GABA, glutamate decarboxylase (GAD). In these mice, however, GFP expression was restricted to subsets of GABAergic neurons (Oliva et al. 2000; Chattopadhyaya et al. 2004; Lopez-Bendito et al. 2004; Ma et al. 2006). In GAD67-GFP knock-in mice, the overall GABA content was shown to be reduced following destruction of the endogenous GAD67 gene (Tamamaki et al. 2003). Bacterial artificial chromosome (BAC) technology has gradually come to be regarded as a potent method to identify and manipulate specific neuron types in mice (Heintz 2001; Meyer et al. 2002), but its application in rats has not previously been reported. In this study we have, for the first time, produced transgenic rats that have both fluorescent labeling of nearly all cortical GABAergic cells and normal levels of GABA synthesis, thus facilitating the study of GABAergic neurons in tissue that is otherwise physiologically normal. To do this we used a BAC containing 2 genes: one for VGAT, which is responsible for transporting GABA into synaptic vesicles (Ebihara et al. 2003), and another for Venus, a fluorescent marker much brighter than

eGFP (Nagai et al. 2002). This manipulation generated 2 lines of VGAT-Venus transgenic rats from the same BAC construct. We show that in at least one of the 2 lines, GABAergic cells in individual areas in the forebrain are selectively labeled with Venus. In the cerebral cortex almost all Venus-expressing cells in both lines were positive for GABA, and the vast majority expressed at least one of 6 chemical markers used to classify cortical interneurons. Venus labeling facilitated the identification of GABAergic cells and made possible targeted recording of the interneurons with morphological features typical of pyramidal cells.

Materials and Methods

Identification of a Suitable BAC Clone

A BAC clone (#160L22) from a 129SV mouse genomic BAC library (Genome System, St Louis, MO), containing the VGAT gene was identified by PCR as previously described (Ebihara et al. 2003). We determined the nucleotide sequences of the 5′- and 3′-termini of the DNA inserted into the BAC vector and compared their sequences with the EMBL database (accession number AL663091). The comparison revealed that BAC clone #160L22 contains the entire VGAT gene, with an additional 102 and 25 kb of DNA flanking the 5′ end of exon 1 and the 3′ end of exon 3, respectively.

Modification of the BAC Clone

pCS2-Venus, which contains Venus complementary DNA (cDNA) followed by the SV40 polyadenylation signals, was generously provided by Dr A. Miyawaki (RIKEN, Wako, Japan) (Nagai et al. 2002). pKOV-Kan and pDF25 plasmids were a generous gift from Dr M. D. Lalioti (University of Birmingham, Birmingham, UK).

The multiple cloning site following the SV40 polyadenylation signals of pCS2-Venus was changed to a *Not*I-*Nco*I-*Apa*I site by ligation of a synthetic linker to pCS2-Venus digested with *Not*I and *Apa*I, and the resultant plasmid was named pCS2-Venus-N. A 3.6-kb *Eco*RI fragment containing the 5′-flanking region, exon 1 and part of intron 1 of the mouse VGAT (mVGAT) gene was subcloned into pBluescript II (Stratagene, LaJolla, CA) from a BAC clone encoding the mVGAT gene (Ebihara et al. 2003), and the resultant plasmid was named pBS-VGAT-E1. A 1.0-kb *Nco*I fragment containing the Venus cDNA followed by the SV40 polyadenylation signals (poly-A) was excised from pCS2-Venus-N and inserted into pBS-VGAT-E1 digested with *Nco*I in order to place the Venus cDNA in frame into the ATG translational initiation codon of exon 1 of the VGAT gene. This plasmid was named pBS-VGAT-E1-Venus. The multiple cloning site of pBluescript II was changed to a *Sal*I-*Eco*RI-*Nhe*I-*Bam*HI site by ligation of a synthetic linker to pBluescriptII digested with *Sal*I and *Bam*HI, and the resultant plasmid was named pBS-SENB. A 3.3-kb *Eco*RI/*Nhe*I fragment was excised from pBS-VGAT-E1-Venus and inserted into pBS-SENB, and the resultant plasmid was named pBS-VGAT-EN-Venus. The cloning site of pKOV-Kan was changed to a *Sal*I-*Eco*RI-*Nhe*I-*Bam*HI site by ligation of a synthetic linker to pKOV-Kan digested with *Sal*I and *Bam*HI, and the resultant plasmid was named pKOV-SENB. A 3.3-kb *Eco*RI/*Nhe*I fragment was excised from pBS-VGAT-EN-Venus and inserted into pKOV-SENB, and the resultant plasmid was named pKOV-VGAT-Venus. The shuttle vector pKOV-VGAT-Venus contains the Venus cDNA and SV40 poly-A flanked by 2 homologous regions: one is genomic DNA homologous to 941 bp (*Nhe*I/*Nco*I) upstream of the translation initiation site of exon 1 of the VGAT gene and the other is genomic DNA homologous to 1393 bp (*Nco*I/*Eco*RI) downstream of the VGAT gene.

BAC recombinations were performed according to the methods described by Lalioti and Heath (2001). Venus-modified BAC clones were confirmed by PCR, pulse field gel electrophoresis, and Southern blotting.

Generation of BAC Transgenic Rats

For pronuclear injections, BAC DNA was purified with a NucleoBond BAC100 kit (Macherey-Nagel, Düren, Germany) and digested with *Nru*I to release the VGAT-Venus DNA, which consisted of the entire insert of genomic DNA and part of the vector DNA from the BAC backbone. The 133-kb linearized BAC DNA fragment was purified using pulse field gel electrophoresis, dissolved at a concentration of 3 ng/μL in 10 mM Tris-Cl and 0.1 mM ethylenediaminetetraacetic acid, and then stored at 4 °C. The purified and stored BAC DNA was injected into fertilized eggs of Crlj:Wistar rats (Charles River Japan, Inc., Kanagawa, Japan) according to the procedure described by Takahashi et al. (1999).

Among 318 oocytes injected, 182 could be transferred into pseudo-pregnant female rats. From them, 25 rats were born. Two transgenic founders were identified from 21 pups by PCR for the presence of Venus. Primers used for the PCR were Venus-F: 5′-ATGGTGAGC-AAGGGCGAGGAGCTGT-3′ and Venus-R: 5′-TTACTTGTACAGCTCGTC-CATGCCGA-3′. The lines derived from these 2 founders were expanded for further analysis. Venus expression in both lines of newborn rat brains was detected by fluorescence microscopy.

Measurement of GABA Content

Samples from rat brains were homogenized with 0.1 M perchloric acid to extract amino acids and precipitate proteins. The homogenates were centrifuged at 6000 × *g* for 15 min at 4 °C and then the supernatant was neutralized with 0.1 M sodium carbonate. After addition of sodium carbonate, the samples were filtered by using Ultrafree-MC (Millipore Corp., Bedford, MA). Amino acids in the samples were derivatized with *o*-phthalaldehyde/2-mercaptoethanol reagent, and GABA concentrations were measured by using high performance liquid chromatography (BAS, Tokyo, Japan) and fluorescence detection. Protein concentrations were determined using bicinchoninic acid protein assay reagent (Pierce, Rockford, IL), with bovine serum albumin (BSA) as a standard.

Antibodies

Venus was immunohistochemically detected using a rabbit antiserum against eGFP (1: 2000; kind gift from Dr Nobuaki Tamamaki, Kumamoto University). In the cortex of transgenic rats, Venus fluorescence almost always colocalized with the immunofluorescence by its antibody. For GABA immunohistochemistry, a mouse monoclonal antibody was used (1:500; Chemicon [Temecula, CA] MAB316).

Parvalbumin was visualized by a mouse monoclonal antibody (Sigma [Saint Louis, MO] P-3171; 1:2000) and a rabbit antiserum (Swant, Bellinzona, Switzerland PV-28; 1:4000). Somatostatin was immunohistochemically detected by a rabbit antiserum (antisomatostatin 28; Dr Robert Benoit, S 309; 1:4000) or a rat monoclonal antibody against somatostatin (Chemicon, MAB354; 1:250). Calretinin was detected by a mouse monoclonal antibody (Chemicon, MAB1568; 1:4000) or a rabbit antiserum (Swant, 7699/4; 1:2000, Diasorin, Stillwater, MN). Cholecystokinin (CCK) immunoreactivity was detected by a monoclonal antibody raised against CCK/Gastrin (#28.2 MoAb, CURE/UCLA/DDC Antibody/RIA Core; 1:4000) or a rabbit antiserum against CCK-8 (Sigma, C-2581; 1:1000). These 2 antibodies against the same antigens stained the same populations of cells in the rat frontal cortex. Vasoactive intestinal polypeptide (VIP) was immunohistochemically found by a rabbit antiserum (Diasorin, 20077; 1:2000). Calbindin immunoreaction was done by a rabbit antiserum (anticalbindin D; Dr Piers C. Emson; 1:2000).

The expression pattern of α-actinin-2 was investigated using a rabbit specific antiserum against α-actinin-2 (4B2; kind gift from Dr Alan H. Beggs, Children's Hospital Boston; 1:2000) (Wyszynski et al. 1998) or a mouse monoclonal antibody against α-actinin-2 and -3 (EA53; Sigma, A7811; 1:2000). Because α-actinin-3 is not expressed in the brain, the EA53 antibody should be specific for α-actinin-2 in rat brain (Wyszynski et al. 1998). This was confirmed using double immunofluorescence showing the rabbit antiserum and the monoclonal antibody against α-actinin-2 stain the same population of cells in the rat cortex.

Immunohistochemistry in Perfusion-Fixed Brains

After anesthesia with an overdose of Nembutal, transgenic and wild-type Wistar rats (28–32 days postnatal) were perfused through the heart with 10 mL of a solution of 250 mM sucrose, 5 mM $MgCl_2$ in 0.02 M phosphate buffer (pH 7.4) (PB), followed by 200 mL of fixative containing 4% paraformaldehyde, 0.05% glutaraldehyde, and 0.2% picric acid in 0.1 M PB. For GABA immunohistochemistry, the glutaraldehyde concentration was increased to 0.5%. The brains were then removed and postfixed in the same fixative for 2 h.

For the immunoperoxidase reaction, the brains were cut at thickness of 50 μm by a vibrating slicer, to the frontal, parasagittal, or oblique horizontal (parallel to the rhinal fissure) sections. Sections were incubated with 1% H_2O_2 in PB to suppress intrinsic peroxidase activity. Sections were

incubated overnight in the primary antiserum in 0.05 M Tris-HCl buffered saline (pH 7.6) (TBS) containing 10% normal goat serum (NGS), 2% BSA, and 0.5% TritonX-100 (TX). After washes with TBS, the sections were incubated with biotinylated secondary antiserum (Vector Laboratories [Burlingame, CA] 1: 100) in TBS containing 10% NGS, 2% BSA and 0.5% TX. After additional washes, they were incubated in ABC complex in TBS (1: 100; Vector). After incubation with 0.05 M Tris-HCl buffer (TB), the sections were reacted with 3,3′-diamino-benzidine tetrahydrochloride (DAB) and H_2O_2. After washing in PB, the sections were put on gelatin-coated slides and dried. After further treatment with 0.1% OsO_4, in PB, they were dehydrated and coverslipped with Entellan.

Colocalization between Venus and a substance or pairs of substances was investigated using immunofluorescence with cryostat sections. Fixed brains were put in 15% sucrose in PB overnight followed by 30% sucrose in PB overnight before sectioning on a cryostat. The sections were put on a cryostat and sectioned at thickness of 2 μm for GABA immunohistochemistry and 4 μm for other chemical markers.

For combined single immunofluorescence and Venus observation, sections were washed in TBS and then incubated with a primary antibody in TBS containing 10% NGS, 2% BSA, and 0.5% TX overnight. After washes with TBS, the sections were incubated with an Alexa 594-conjugated secondary antibody (1:200; Molecular Probes, Eugene, OR). For experiments using double immunofluorescence for α-actinin-2 and other markers in wild-type rats, sections were incubated with mouse and rabbit primary antibodies, followed by a mixture of Alexa 488- and Alexa 594-conjugated secondary antibodies. After washing in TBS the sections were mounted on gelatin-coated glass slides and dried. The sections were coverslipped with 50% glycerin in TBS and observed by epifluorescence. Cross-reactivity of the secondary antisera used for dual immunofluorescence was tested by incubating control sections first with a single primary antiserum or monoclonal antibody and then with a secondary antibody appropriate for the different primary applied for double staining.

The following filters were used for fluorescence observation: excitation, 485–515 nm; emission, 525–555 nm for Venus; excitation, 545–580 nm; emission, 610 nm for Alexa 594; excitation, 360–370 nm; emission, 420–460 nm for Alexa 350. Peak absorption and emission of Venus are 515 and 528 nm, respectively (Nagai et al. 2002).

Single- and dual-labeled fluorescent cells were counted directly under a fluorescent microscope or from photomicrographs of sections containing the medial agranular and anterior cingulate cortex. Percentages were calculated from the number of dual-labeled cells (Venus plus GABA) divided by the total population of single-labeled cells (Venus or GABA).

Slice Preparation and Whole-Cell Recording

Oblique horizontal sections with 300 μm thickness were cut along the line of rhinal fissure from rat frontal cortex (19–23 days postnatal), immersed in a buffered solution (NaCl, 124.0; KCl, 3.0; $CaCl_2$, 2.4; $MgCl_2$, 1.2; $NaHCO_3$, 26.0; NaH_2PO_4, 1.0; glucose, 10.0; in mM) aerated with a mixture of 95% O_2 and 5% CO_2. Cells in the frontal cortex (medial agranular and anterior cingulate cortex) were visualized using a 40× water immersion objective, and recorded in whole-cell current-clamp mode at 32 °C. The electrode solution for the current-clamp recording consisted of potassium gluconate 130, NaCl 1.8 $MgCl_2$ 1.8, adenosine triphosphate 2.8, guanosine triphosphate 0.3, 4-(2-hydroxyethyl)-1-piperazineethanesulfonic acid 10, and biocytin 20 mM. The pH of the solution was adjusted to 7.3 with KOH and the osmolarity was adjusted to 290 mOsm. The recorded Venus-expressing cells were observed by direct visual inspection, combined with Nomarski optics, in fluorescence microscope (BX50WI, Olympus, Tokyo, Japan). Current-clamp recordings were made in a fast current-clamp mode of EPC9/dual (HEKA, Lambrecht/Pfalz, Germany; WaveMetrics, Lake Oswego, OR). Electrophysiological data were analyzed by IGOR Pro (WaveMtrics). Cellular input resistance was determined from the membrane response to small hyperpolarizing current injections (<100 pA, 0.5 s duration). Spike widths at half amplitude were measured from spikes elicited by brief (10 ms) depolarizing current injections, whereas the presence of low-threshold (LTS) or burst-spiking behavior was assessed using just-threshold current injection from a starting potential of −75 to −85 mV.

Physiological Identification of Nonpyramidal Cells

Cortical nonpyramidal cells are physiologically heterogeneous and have been classified according to their patterns of action potential generation in response to depolarizing current pulses, and have been divided into 3 broad subclasses: fast-spiking (FS) cells, late-spiking (LS) cells, and non-FS neurons (Kawaguchi and Kubota 1997; Kawaguchi and Kondo 2002; Karube et al. 2004). FS cells are characterized by nonadapting, repetitive spike discharges at a threshold frequency of 40–150 Hz. At just-threshold current levels, FS cell discharges consist of either single spikes at the beginning of the current pulse or irregular bursts of high frequency spike generation with constant spike intervals interspersed. LS cells are characterized by a slow ramp depolarization and delayed action potential firing following just-threshold current injections. Non-FS cells are more heterogeneous in their electrophysiological characteristics than are FS and LS neurons. Some common non-FS cells are LTS neurons (also known as burst-spiking nonpyramidal [BSNP] neurons), regular-spiking nonpyramidal (RSNP) cells, and irregularly spiking neurons, which we have classified here as either BSNP or RSNP cells according to the presence of an initial LTS-like hump (Kawaguchi and Kubota 1996).

Immunohistochemical and Morphological Analysis of Recorded Cells

Tissue slices containing biocytin-loaded cells were fixed by immersion in 4% paraformaldehyde and 0.2% picric acid overnight, followed by a freeze-thawing procedure in sucrose-containing PB using liquid nitrogen twice. Slices were resectioned to a thickness of 50 μm, and were processed for fluorescence immunohistochemistry. Slices were incubated with a primary antibody in TBS containing 2% BSA, 10% NGS, and 0.1% TX. The primary antibody was antiparvalbumin (mouse; 1:4000), antisomatostatin (rat; 1:250), or anti-α-actinin-2 (mouse monoclonal; 1:100,000). After washing in TBS, they were incubated in a Alexa 594-conjugated secondary antibody in TBS containing BSA, NGS, and 0.1% TX for 2 h, followed by incubation with Alexa 350 streptavidin (1:4000; S-11249, Molecular Probes) in TBS for 40 min. After examination for fluorescence, the slices were incubated with ABC complex in TBS containing 0.04% TX, and reacted with DAB and H_2O_2 in TB. They were then postfixed in 1% OsO_4 in PB for 20 min, dehydrated, and flat-embedded on glass slides in Epon. Somata, axons, and dendrites were reconstructed 3-dimensionally using the Neurolucida system (MicroBrightField, Williston, VT). The proportion of boutons in apposition with other somata was calculated from more than 200 randomly sampled boutons.

Data are given as mean ± standard deviation (SD). Analysis of variance (ANOVA) was used for confirmation of significant differences among subtypes in individual parameters, followed by post hoc Tukey test for the group comparison.

Results

Generation of BAC Transgenic Rats

A BAC construct harboring a modified VGAT allele (Fig. 1*A*) was made as described in the Methods. The modified BAC construct included 102 kb upstream of the VGAT gene, and 25 kb downstream. As the VGAT gene itself is only 5 kb (Ebihara et al. 2003), all of the VGAT gene's regulatory regions are likely included within the BAC. Although eGFP is a well-known in vivo marker, we used Venus, a derivative of yellow fluorescent protein (YFP), in place of eGFP because of its enhanced fluorescence (~20-fold brighter than eGFP; Nagai et al. 2002).

Two founder rat lines carrying the VGAT-Venus transgenes were identified by PCR analysis and maintained on a Wistar background. Both lines (lines A and B) transmitted the transgene to their progeny, and lines A and B were named VGAT-Venus-A and VGAT-Venus-B, respectively. Both lines of transgenic rats were characterized for transgene expression, and Venus expression could be observed at postnatal days 1–2 through the skin and skull by fluorescence microscopy.

Both lines of VGAT-Venus transgenic rats exhibit normal growth and reproductive behavior. To confirm the normal production of GABA, we compared the GABA content to total

protein in the cerebrum and cerebellum in VGAT-Venus transgenic rats and their Venus-negative littermates (taking the means of wild-type rats as 100%). VGAT-Venus-A expressing brains had a GABA content ($n = 7$; 103.7 ± 11.3% in cerebrum; 101.3 ± 14.4 in cerebellum) similar to that found in wild-type littermates ($n = 7$; 100.0 ± 8.4% in cerebrum and 100.0 ± 11.4 in cerebellum). VGAT-Venus-B brains also contained similar GABA content ($n = 6$; 103.1 ± 10.1% in cerebrum; 96.7 ± 12.2% in cerebellum) to that of their wild-type littermates ($n = 6$; 100.0 ± 10.3% in cerebrum and 100.0 ± 15.9 in cerebellum). In addition to having normal GABA, the brain structures of both lines showed no abnormalities at the macroscopic level (Fig. 2), and in sections from fixed brains we observed many fluorescent cells. Fluorescence was evident not only in somata, but also in dendrites and axonal boutons (Fig. 1*B–D*).

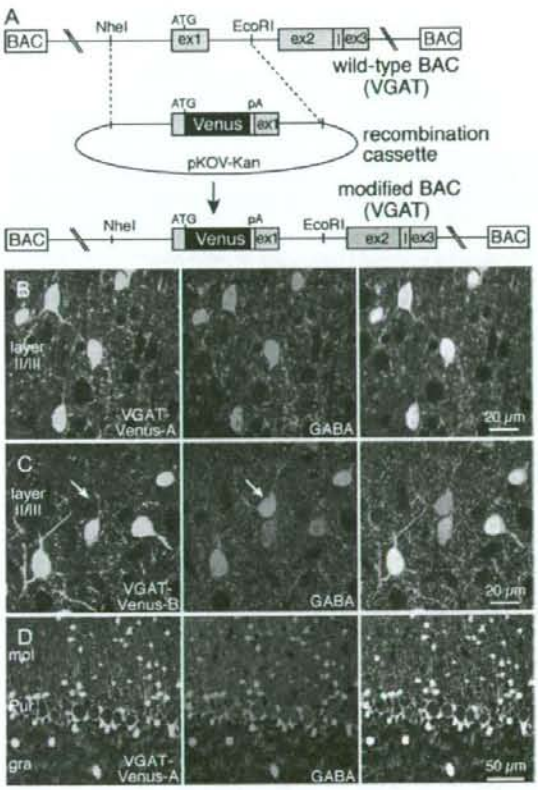

Figure 1. Generation of BAC transgenic rats with Venus fluorescence in VGAT (vesicular GABA transporter)–expressing neurons. (*A*) Schematic representation of the structure of BAC #160L22 containing the VGAT gene (top; wild-type BAC), the recombination cassette (middle), and the modified BAC (bottom). Venus cDNA followed by a poly-A signal was placed into exon 1 of the VGAT gene in frame with the translational initiation codon, ATG. (*B–D*) Colocalization of Venus fluorescence and GABA immunoreactivity in the cerebral and cerebellar cortex of VGAT-Venus transgenic rats. (*B*) Venus-positive cells (left) almost completely overlapped with the GABA-positive population (middle) in layer II/III of the frontal cortex in the "A" line of VGAT-Venus (VGAT-Venus-A) rats. The 2 fluorescence images are merged at the right. (*C*) Venus-positive cells (left) mostly overlapped with the GABA-positive population (middle) in the "B" line of VGAT-Venus (VGAT-Venus-B) rats. However, a few cells were positive for GABA but not for Venus (arrow). The 2 fluorescence images are merged at the right. (*D*) Venus-positive cells (left) in the molecular and granular layer of the cerebellar cortex almost completely overlapped with the GABA-positive population (middle) in VGAT-Venus-A rats, whereas Purkinje cells displayed little Venus fluorescence. GABA immunofluorescence was also weak in Purkinje somata. Abbreviations: mol, molecular layer; Pur, Purkinje cell layer; gra, granule cell layer.

Venus Expression Patterns

To confirm whether Venus-expressing cells are also GABAergic in the neocortex, Venus and GABA immunofluorescence were compared in the frontal cortex (Fig. 1*B–D*). About 98% of Venus-positive cells in line A- and ~95% of Venus-positive cells in line B-animals were also positive for GABA (Table 1). Conversely, in line A, almost all GABA cells displayed Venus fluorescence (Fig. 1*B*), indicating GABA and Venus cells comprise almost completely overlapping populations of neurons in the frontal cortex (Table 1). On the other hand, in the B line, GABA-positive cells in deeper cortical layers were mostly positive for Venus, but some GABAergic cells in the superficial layers, especially layer I, did not express Venus (Fig. 1*C*). This indicates that Venus-positive cells in the frontal cortex of VGAT-Venus-B rats are GABAergic, but that not all GABAergic cells express Venus, especially in layer I (Table 1).

Colocalization of Venus and GABA immunofluorescence was also investigated in the cerebellar cortex of VGAT-Venus-A animals. In the granule cell layer, a few large, putative Golgi cells, had Venus fluorescence that completely overlapped with GABA immunofluorescence (38 cells positive for both Venus and GABA; Fig. 1*D*). Venus cells in the molecular layer also greatly overlapped with GABA-positive cells (484 Venus cells among 492 GABA cells, 98.4%). In contrast, GABAergic Purkinje cells showed only weak Venus fluorescence. GABA immunofluorescence was also weak at their somata (Fig. 1*D*). These data indicate that GABAergic interneurons and Venus cells show a high degree of overlap in the cerebral and cerebellar cortices of transgenic rats, especially in the A line, which had an almost complete overlap of GABA-positive and Venus-positive neurons.

We next compared the Venus and GABA expression patterns in the 2 VGAT-Venus lines, and in wild-type rats, in various brain regions using specific antibodies and DAB staining (Figs 2 and 3).

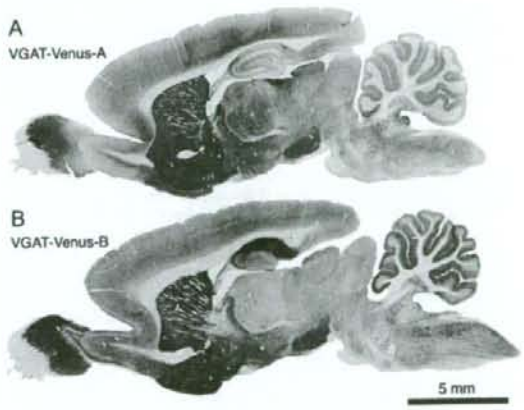

Figure 2. Distribution patterns of Venus in VGAT-Venus rats. Venus was visualized in parasagittal brain slices using the antibody and peroxidase DAB reaction. (*A*) Venus expression in a VGAT-Venus-A rat. (*B*) Venus expression in a VGAT-Venus-B rat. In the forebrain, Venus distribution was similar to that of GABA, except in the hippocampal CA1 region in VGAT-Venus-B rats and thalamus in VGAT-Venus-A rats.

Neocortex

As was found in the frontal cortex, described above, other cortical regions in both animal lines had Venus-positive cells in all layers. In A line animals, Venus cells in layers I–V were positive for GABA. In addition to the expected GABA-positive neurons, layer VI of nonfrontal cortical regions also had some neurons that were faintly labeled with Venus but negative for GABA. In the B line, Venus-expressing cells in layers I–VI were positive for GABA. In addition, in B line animals, a few pyramidal cells in the ventral cortex showed weak Venus fluorescence but were negative for GABA.

Table 1
Relation of Venus fluorescent cells and GABA immunopositive cells in frontal cortex

	VGAT-Venus-A		VGAT-Venus-B	
Layer	Venus/GABA	GABA/Venus	Venus/GABA	GABA/Venus
I	98.6 ± 1.4 (148)	100 ± 0.0 (146)	55.3 ± 4.2 (153)	99.4 ± 1.1 (88)
II/III	97.3 ± 3.6 (1387)	98.6 ± 2.3 (1364)	93.7 ± 0.3 (1551)	98.5 ± 0.7 (1477)
V	97.7 ± 2.5 (1075)	98.5 ± 2.0 (1064)	98.9 ± 0.3 (998)	98.1 ± 2.4 (1011)
VI	98.0 ± 2.1 (1172)	98.7 ± 1.5 (1163)	98.9 ± 0.4 (1342)	99.1 ± 0.8 (1347)
Total	97.6 ± 2.8 (3782)	98.7 ± 1.8 (3737)	95.3 ± 0.5 (4044)	98.7 ± 1.1 (3923)

Note: Data are percentages and mean ± SD of 3 animals. (), total numbers of GABA or Venus cells of 3 VGAT-Venus-A or -B rats.

Hippocampus

In VGAT-Venus-A rats, nonpyramidal cells were labeled with Venus, but no Venus was detected in pyramidal cells in the CA1–3 regions, or in granule cells in the dentate gyrus (Fig. 3*A*), indicating that Venus cells overlap with GABAergic neurons. In VGAT-Venus-B rats, nonpyramidal cells were selectively labeled with Venus in CA2, CA3, and dentate gyrus, but in CA1 both pyramidal and nonpyramidal cells showed fluorescence at their somata and dendrites (Fig. 3*B*).

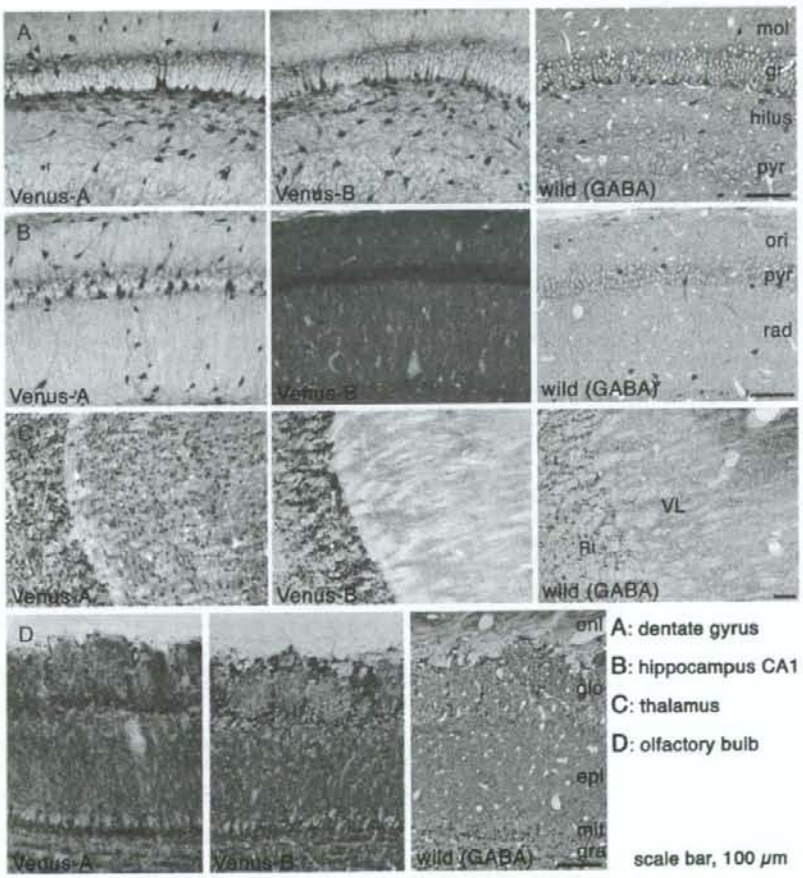

Figure 3. Comparative distribution of Venus-positive cells in 2 lines of VGAT-Venus rats and GABA-positive cells in wild-type rats. Venus expression was more clearly seen in somata than was GABA immunoreactivity. (*A*) Dentate gyrus and CA3 region of the hippocampus: nonpyramidal cells, but not granule or pyramidal cells, expressed Venus in both animal lines. (*B*) CA1 regions of the hippocampus: only nonpyramidal cells expressed Venus in the VGAT-Venus-A rat, but pyramidal cells also expressed Venus in the VGAT-Venus-B rat. (*C*) Thalamus: reticular nucleus cells expressed Venus in both lines of VGAT-Venus rats, but Venus was found in other nucleus in the VGAT-Venus-A rats. (*D*) Olfactory bulb: periglomerular and granule cells were stained in both lines. In the external plexiform layer, dendrites of granule cells were stained. Abbreviations: mol, stratum moleculare; gr, stratum granulare; pyr, stratum pyramidale; ori, stratum oriens; rad, stratum radiatum; Rt, reticular nucleus; VL, ventrolateral nucleus; onl, olfactory nerve layer; glo, glomerular layer; epl, external plexiform layer; mit, mitral cell layer; gra, granular layer.

Thalamus

Venus expression was found in the GABAergic reticular nucleus of both lines (Fig. 3*C*). Further, the lateral geniculate nuclei in both lines contained Venus-positive cells that likely correspond to GABAergic interneurons. In VGAT-Venus-A rats, Venus-positive cells were also found in projection neurons (likely glutamatergic) in other thalamic nuclei such as the ventrolateral, ventroposterior, and laterodorsal nuclei. Thalamic projection cells were not labeled with Venus in VGAT-Venus-B rats.

Olfactory Bulb

Excitatory mitral and tufted cells did not express Venus, whereas granule and periglomerular cells, considered to be GABAergic, were labeled with Venus (Fig. 3*D*). In the granule and inner plexiform layers, a few Venus-positive large cells existed, perhaps corresponding to so-called "short axon cells." The external plexiform layer also had a few large Venus-positive cells that may also belong to the short axon cell group or to other unidentified subtypes. No differences were found in the distribution patterns of Venus-positive cells between the 2 lines.

Basal Ganglia Nuclei

Venus was expressed in GABAergic cells in the basal ganglia of both VGAT-Venus-A and -B animals. In the striatum most cells expressed Venus, indicating labeling of GABAergic projection cells. Qualitatively, most parvalbumin, somatostatin, and calretinin cells were fluorescently labeled in VGAT-Venus-A rats, but large cells positive for choline acetyltransferase were devoid of Venus. Parvalbumin cells showed stronger fluorescence than other types. In both the globus pallidus and entopeduncular nucleus, large multipolar cells were labeled with Venus, corresponding to GABAergic principal cells. The subthalamus showed no Venus fluorescence, whereas many Venus cells were found in zona incerta. In the substantia nigra, the pars reticulata had many Venus cells, corresponding to GABAergic output cells, whereas no Venus cells were localized in the dopaminergic neurons of the pars compacta.

Venus in Cortical GABA Cell Subtypes

To determine whether various GABAergic cell subtypes were labeled with Venus, we investigated colocalization patterns of Venus with the chemical markers for cortical GABAergic cells: parvalbumin, somatostatin, VIP, CCK (Fig. 4*A–D*). Further, we examined the colocalization of Venus and α-actinin-2, an actin-binding protein expressed by some GABAergic neurons in the hippocampus (Ratzliff and Soltesz 2001). In VGAT-Venus-A rats, α-actinin-2–positive cells in all layers also expressed Venus (100% in all layers; Table 2), suggesting that all α-actinin-2–positive cells are GABAergic (Fig. 4*F*). Calretinin is also expressed in GABAergic neurons (Kubota et al. 1994), but we found calretinin immunofluorescence to be variable in intensity. Most cells with strong immunofluorescence also had Venus fluorescence, but some cells with weaker labeling were devoid of Venus in VGAT-Venus-A rats (Fig. 4*E*), suggesting that some non-GABAergic cells may express calretinin (Melchitzky et al. 2005). Therefore, Venus expression was quantitatively analyzed for colocalization with biochemical markers other than calretinin (Table 2). However, we also calculated the proportion of cells expressing all of the above biochemical markers, including calretinin, among the total Venus-positive population (Table 3).

In VGAT-Venus-A rats, cells positive for parvalbumin, somatostatin, VIP, CCK, or α-actinin-2 were almost always positive for Venus (Table 2). This result is consistent with the finding that Venus cells overlap fully with GABAergic cells in the VGAT-Venus-A line. In VGAT-Venus-B rats, the vast majority of parvalbumin and somatostatin cells were also positive for Venus, but a few VIP and CCK cells, and many α-actinin-2 cells were negative for Venus (Table 2). These data suggest that GABAergic cells negative for Venus in VGAT-Venus-B correspond to subpopulations of VIP, CCK, and especially α-actinin-2 cells.

Composition of Cortical GABAergic Population

Because the Venus-positive neuron population overlapped completely with GABA immunoreactivity in VGAT-Venus-A rats, we were able to measure the proportion of each chemical subtype in the total GABAergic (Venus-positive) population in 3 rats. This method, using Venus-expressing tissue, was found to be both easier and more reliable than doing double immunostaining with antibodies to both GABA and a second chemical marker (Fig. 4*A–F*). The mean values obtained from 3 rats are shown in Table 3 and Figure 4*G*. Parvalbumin-positive cells were not found in layer I neurons expressing Venus, but made up 36.4% of Venus-positive cells in layer II/III, 52.7% of cells in layer V, and 38.7% of cells in layer VI. Somatostatin-positive cells were not found in layer I Venus-positive cells, but made up 17.4% of cells in layer II/III, 28.6% of cells in layer V, and 29.0% of cells in layer VI. VIP-positive cells made up 3.3% of layer I Venus-positive cells, 24.0% of cells in layer II/III, 9.6% of cells in layer V, and 8.0% of cells in layer VI. Calretinin cells comprised 35.8% of Venus cells in layer I, 21.0% of cells in layer II/III, 11.1% of cells in layer V, and 11.4% of cells in layer VI. CCK was found in just 0.9% of cells in layer I, 8.9% of cells in layer II/III, 2.9% of cells in layer V, and 3.0% of cells in layer VI. Finally, α-actinin-2–positive cells comprised 66.5% of Venus-positive cells in layer I, 9.8% of cells in layer II/III, 1.5% of cells in layer V, and 6.2% of cells in layer VI.

To estimate the proportion of all GABAergic cells expressing the above 6 chemical markers, their colocalization patterns should be known. Parvalbumin and somatostatin cells were completely independent groups and were also devoid of the other 3 chemical markers (Kubota et al. 1994; Gonchar and Burkhalter 1997; Kubota and Kawaguchi 1997). Coexistence of calretinin and CCK was found in a few cells. Among VIP-positive cells, calretinin was expressed in 33% in layer II/III, 71% in layer V, and 54% in layer VI. Among VIP-positive cells, CCK was expressed in 32% in layer II/III, 21% in layer V, and 19% in layer VI (Kubota and Kawaguchi 1997 and related unpublished observations). Results of the α-actinin-2 colocalization with the other chemical markers in wild-type rats are available in the Appendix below (Fig. 8, Table 5). Parvalbumin-positive and somatostatin-positive cells did not express α-actinin-2, and only a very few VIP-positive and CCK-positive neurons were positive for α-actinin-2. Some α-actinin-2–positive cells showed calretinin immunoreactivity, especially in layer I (14.8%), layer V (18.8%) and layer VI (16.2%). Assuming the colocalization of α-actinin-2 and calretinin in addition to the previously revealed relationships, these 6 chemical markers cover more than 90% of the total GABAergic populations in layers I, II/III, and V, and nearly 90% of cells in VI (Fig. 4*G*).

Functional Characteristics of Venus Cells

To determine whether Venus-expressing cells have differentiated normally into GABAergic cell subtypes, Venus-positive cells

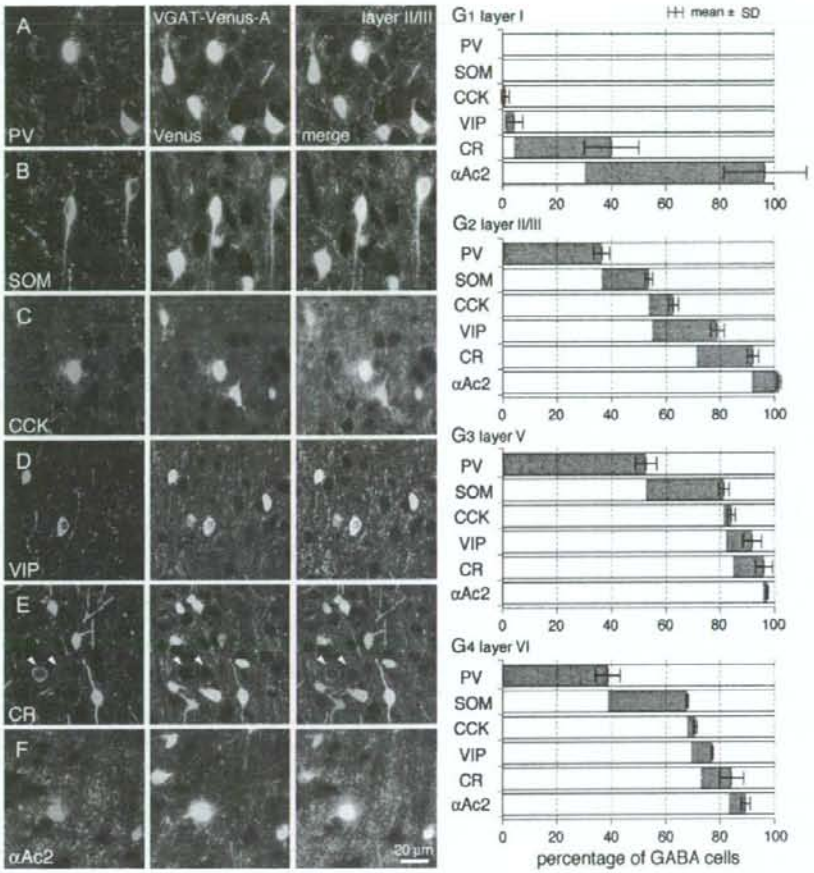

Figure 4. Chemical composition of cortical GABAergic population. (*A–F*) Venus expression in chemically identified cells in layer II/III of VGAT-Venus-A rats. (*A*) Photomicrographs from the same microscopic field, showing the relationship of parvalbumin (PV) and Venus cells. (*B*) Somatostatin (SOM) cells. (*C*) CCK cells. (*D*) VIP cells. (*E*) Calretinin (CR) cells. (*F*) α-Actinin-2 (αAc2) cells. Almost all cells positive for markers other than calretinin expressed Venus. Some calretinin cells (arrows) showed no Venus fluorescence. Calretinin immunofluorescence in these non-Venus labeled neurons was generally weaker than in cells expressing Venus. (*G*) Graph showing the proportion of GABAergic neurons found to express specific chemical markers, including α-actinin-2 (αAc2) cells. The proportion was calculated from 3 VGAT-Venus-A rats. (*G1*) Layer I. (*G2*) Layer II/III. (*G3*), Layer V. (*G4*) Layer VI. Individual bars were displaced to show the overlap in the colocalized portion with another marker. Considering the colocalization patterns of the 6 markers, more than 90% of GABA cells were found to express at least one of the 6 chemical markers in layers I, II/III, and V.

in the cortex were examined for their physiological, morphological, and chemical characteristics (Kawaguchi and Kondo 2002). In layer V of the frontal cortex of VGAT-Venus-A rats, we made whole-cell recordings from FS, RSNP, and BSNP cells. Among 12 recorded FS cells in layer V, 11 cells showed parvalbumin immunoreactivity (Fig. 5*A*), of which 9 cells were identified as basket cells with similar morphology to cells in the wild-type animals (Fig. 5*C2,D*). The remaining 3 FS cells were not morphologically identified because of poor axonal staining. Seven RSNP cells in layer V were immunoreactive for somatostatin, of which 5 cells were Martinotti cells with ascending axonal arbors similar to those found in wild-type rats. Of 8 somatostatin-positive BSNP cells, 6 had morphologies consistent with Martinotti cells (Fig. 5*C1*). Parvalbumin-positive FS cells had more negative resting potentials, smaller input resistances, and shorter spike widths than did somatostatin-positive cells (Table 4), and somatostatin-positive BSNP cells had larger input resistances than RSNP cells (Kawaguchi and Kubota 1996).

To confirm the differentiation of VIP cells, we identified 5 Venus-expressing VIP-positive cells in layer II/III (Fig. 6*A*), among which 2 cells well stained showed the descending axonal arbors morphologically. Physiologically, they included cells with either strong firing adaptation or irregular spiking (Fig. 6*B,C*), and were classified as either RSNP or BSNP. Thus, we found no differences in the physiological, chemical, and morphological characteristics between wild-type and VGAT-Venus rat. These data suggest normal functional differentiation of cortical GABAergic cells in VGAT-Venus rats.

Although most GABAergic cell subtypes can be labeled with calcium-binding proteins and neuropeptides, specific chemical markers have not previously been identified in neocortical LS

neurogliaform cells. In hippocampus, α-actinin-2 is expressed not only in dendrites of pyramidal cells, but also in somata of interneurons (Wyszynski et al. 1998; Ratzliff and Soltesz 2001), including neurogliaform cells (Price et al. 2005). We investigated whether LS cells coincide with the α-actinin-2-positive cell population in frontal cortex. Immunofluorescence for α-actinin-2 was investigated in LS cells whose somata were well stained (n = 6 in layer II/III and n = 2 in layer V). Five LS cells were positive for α-actinin-2 in layer II/III and both positive in layer V (Fig. 5*B*,*C*3). LS neurogliaform cells positive for α-actinin-2 had more hyperpolarized resting potentials than somatostatin cells, longer spike widths than parvalbumin FS cells, and lower input resistances than somatostatin BSNP cells (Table 4).

To further reveal the functional differentiation between parvalbumin, somatostatin, and α-actinin-2 cells, we compared their firing characteristics quantitatively. Parvalbumin FS cells required more current to induce spikes than was required in α-actinin-2 LS cells or somatostatin BSNP cells (Fig. 5*E*). When depolarized just above action potential threshold, parvalbumin and α-actinin-2 cells fired spikes at relatively constant intervals, whereas somatostatin cells showed spike-frequency adaptation. Parvalbumin-positive FS, somatostatin-positive RSNP, and α-actinin-2-positive LS cells increased their firing rate linearly with larger amplitude current injections (up to 500 pA) (Fig. 5*F*). The slope of firing frequency verses injected current (duration, 0.5 s) was 270 Hz/nA in parvalbumin FS cells (correlation coefficient [c.c.] = 0.65), 163 Hz/nA in somatostatin RSNP cells (c.c. = 0.92), and 34 Hz/nA in α-actinin-2 LS cells (c.c. = 0.65), indicating significant differences in the output characteristics of these neurons.

Table 2
Colocalization of chemical markers for GABAergic nonpyramidal cells with Venus in frontal cortex of VGAT-Venus rats

Layer	PV	SOM	VIP	CCK	αAc2
VGAT-Venus-A					
I	No cells	No cells	100% (6)	100% (4)	100% (104)
II/III	99.8% (470)	98.6% (142)	98.3% (359)	100% (165)	100% (154)
V	100% (378)	96.2% (132)	98.8% (85)	100% (28)	100% (15)
VI	99.7% (306)	98.1% (211)	97.6% (85)	97.7% (43)	100% (52)
Total	99.8% (1154)	97.7% (485)	98.3% (535)	99.6% (240)	100% (325)
VGAT-Venus-B					
I	No cells	No cells	28.6% (7)	0.0% (1)	47.0% (134)
II/III	99.7% (622)	98.2% (336)	88.5% (226)	88.9% (235)	59.6% (136)
V	99.9% (731)	98.8% (248)	95.0% (60)	82.9% (41)	85.7% (14)
VI	99.7% (751)	98.4% (189)	95.1% (61)	94.8% (58)	74.5% (47)
Total	99.8% (2104)	98.4% (773)	89.5% (354)	89.0% (335)	57.7% (331)

Note: Venus cells/cells positive for a chemical marker. Data are combined from 3 animals in A line, 2 animals in B line. ( ), number of cells positive for individual chemical markers (denominator). PV, parvalbumin; SOM, somatostatin; αAc2, α-actinin-2.

To assess further the differentiation of Venus-expressing GABAergic cells, we examined the dendritic morphology and synaptic innervation patterns of neurons exhibiting physiological and chemical correlations. The number of dendrites issuing from the soma (primary dendrites) was 6.2 ± 1.6 (n = 9; range, 4–9) in parvalbumin-positive FS basket cells, 6.0 ± 1.8 (n = 6; range, 4–9) in α-actinin-2-positive LS neurogliaform cells, and 3.2 ± 0.8 (n = 11; range, 2–4) in somatostatin-positive Martinotti cells (which were significantly fewer than in the above FS and LS cells, $P < 0.01$).

In a previous study, we used electron microscopy to confirm that about 80% of visually identified (via light microscopy) nonpyramidal neuron axonal boutons apposed to somata make synaptic junctions onto them (Karube et al. 2004). Here we also used Nomarski optics to identify appositions of intracellularly stained axonal boutons onto unstained postsynaptic somata (Fig. 5*D*). For 3 nonpyramidal cell subtypes (FS, Martinotti, and LS cells), we measured the number of stained boutons apposed to other somata as a proportion of the total number of boutons observed. Boutons arising from parvalbumin-positive FS basket cells and somatostatin-positive Martinotti cells targeted somata in 22.3 ± 4.3% and 2.5 ± 1.9%, respectively ($P < 0.01$; Fig. 5*G*). The proportion of somatic apposition in boutons from α-actinin-2-positive LS neurogliaform cells was 14.3 ± 6.4% (larger than the above somatostatin Martinotti cells, $P < 0.01$; smaller than the above parvalbumin FS cells, $P < 0.05$) (Fig. 5*G*), and in addition showed more variability within its group than other subtypes. A comparison of these results with those of wild-type rats is available in the Appendix (Fig. 9), and confirms that the proportion of soma-targeting boutons is similar in wild-type and VGAT-Venus rats. These observations suggest that α-actinin-2-positive LS neurogliaform cells are unique compared with the other cell subtypes in the aspects of physiology, dendritic elongation and innervation targets.

FS Basket Cells Heterogeneous in their Somatic Size and Dendritic Territory

When recording in wild-type rats, we identified cortical GABAergic nonpyramidal cells on the basis of their somatic shape and size. Layer V contains a few large nonpyramidal cells with somatic sizes comparable with pyramidal cells, or having pyramid-shaped somata (Marin-Padilla 1969; Jones 1975; DeFelipe et al. 1986). This has made discriminating these large nonpyramidal cells from the abundant population of pyramidal cells difficult. Although their number is small, large interneurons may play an important role in cortical function (Hensch 2005). Recording from slices of VGAT-Venus rat, we found large FS cells that were of similar size or shape to pyramidal cells (Fig. 7*A*). The maximum cross-sectional areas of layer V FS cells recorded from Venus rats were 220 ± 67 μm^2 (maximum = 356

Table 3
Mean percentages of cells positive for individual chemical markers among Venus cells of frontal cortex in 3 VGAT-Venus-A rats

Layer	PV	SOM	VIP	CR	CCK	αAc2
I	No cells (118)	No cells (63)	3.3 ± 3.2 (121)	35.8 ± 10.1 (78)	0.9 ± 1.5 (214)	66.5 ± 15.2 (173)
II/III	36.4 ± 2.9 (1284)	17.4 ± 1.4 (828)	24.0 ± 2.5 (1473)	21.0 ± 2.1 (1236)	8.9 ± 1.8 (1972)	9.8 ± 0.8 (1579)
V	52.7 ± 3.9 (726)	28.6 ± 1.9 (450)	9.6 ± 3.5 (857)	11.1 ± 3.1 (576)	2.9 ± 1.5 (1096)	1.5 ± 0.4 (1003)
VI	38.7 ± 4.6 (801)	29.0 ± 0.4 (713)	8.0 ± 0.3 (1048)	11.4 ± 4.4 (907)	3.0 ± 0.7 (1437)	6.2 ± 1.6 (847)
Total	39.3 ± 1.4 (2929)	23.4 ± 1.3 (2054)	15.0 ± 0.7 (3499)	16.1 ± 2.7 (2797)	5.5 ± 1.1 (4719)	8.9 ± 1.2 (3602)

Note: Mean ± SD of 3 VGAT-Venus-A rats. PV, parvalbumin; SOM, somatostatin; CR, calretinin; αAc2, α-actinin-2. (), total numbers of Venus cells of 3 VGAT-Venus-A rats.

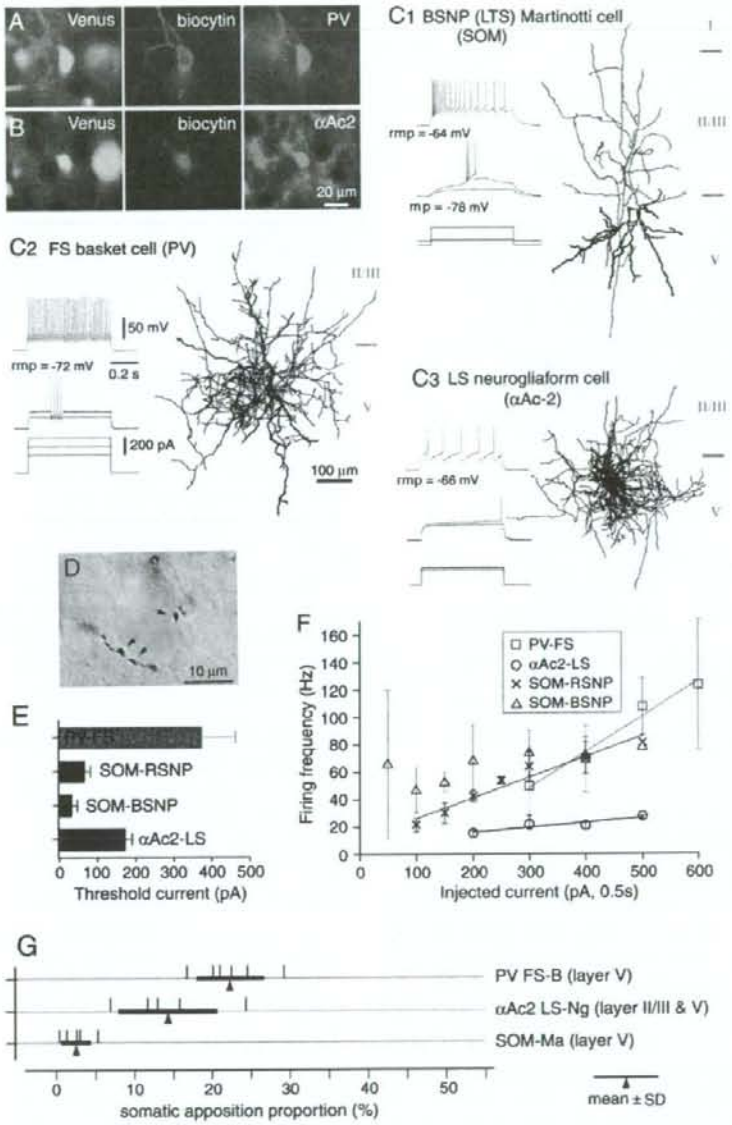

Figure 5. Correlation of physiological, chemical, and morphological characteristics in Venus-expressing cells. (A,B) Immunohistochemical identification of electrically recorded Venus cells labeled by biocytin as parvalbumin- (PV) or α-actinin-2- (αAc2) positive, respectively. (*C*) Firing patterns and morphologies of layer V Venus cells. Somata and dendrites are shown in black, and axons in red. (*C1*) a somatostatin (SOM)-positive BSNP Martinotti cell. LTS was induced from a hyperpolarized potential generated by d.c. somatic current injection (−37 pA). (*C2*) a parvalbumin-positive FS basket cell. (*C3*) an α-actinin-2–positive LS neurogliaform cell. (*D*) Bouton appositions of a Venus- and parvalbumin-positive FS basket cell onto another unstained soma (arrows). (*E*) Threshold currents necessary to induce spikes in response to depolarizing pulses. (*F*) Relationship between firing frequency and current strength. Firing frequency was calculated from the median of spike intervals in response to depolarizing current pulses with duration of 0.5 s. Solid lines indicate simple regression fits for parvalbumin-positive FS, α-actinin-2–positive LS, and somatostatin-positive RSNP cells. (*G*) Comparisons of the proportion of axonal boutons making appositions onto somata in the different nonpyramidal cell types in VGAT-Venus rats. Three subtypes were investigated: 6 parvalbumin-positive FS basket cells (layer V), 5 somatostatin-positive Martinotti cells (layer V), and 5 α-actinin-2–positive LS neurogliaform cells (3 in layer II/III and 2 in layer V). A comparison of these proportions of VGAT-Venus rats with those of wild-type rats is available in the Fig. 9. Abbreviations: mp, membrane potential; rmp, resting mp.

μm^2, $n = 21$; Fig. 7*B*), somewhat larger than those recorded in slices from wild-type rats (131 ± 34 μm^2, maximum = 202 μm^2, $n = 14$) (Kawaguchi et al. 2006), and included cells with similar size to layer V pyramidal cells in the same cortical regions (pyramidal cells projecting to the contralateral striatum, 224 ± 60 μm^2, maximum = 396 μm^2, $n = 19$; pyramidal cells projecting to the pons, 262 ± 45 μm^2, maximum = 360 μm^2, $n = 9$) (Morishima and Kawaguchi 2006). The use of VGAT-Venus rats

Table 4
Electrophysiological properties of nonpyramidal cell subtypes in frontal cortex of VGAT-Venus rats

Cell type	*N*	Resting potential (mV)	Input resistance (M)	Spike half-width (ms)	Threshold current[a] (pA)
PV-FS cells (layer V)	11	−71 ± 3	73 ± 15	0.41 ± 0.07	378 ± 88
SOM-RSNP cells (layer V)	7	−62 ± 3	170 ± 40	0.57 ± 0.04	71 ± 37
SOM-BSNP cells (layer V)	8	−60 ± 4	417 ± 138	0.6 ± 0.12	38 ± 33
αAc2-LS cells (layer II/III, V)	6[b]	−68 ± 2	126 ± 26	0.69 ± 0.06	178 ± 39
ANOVA/post hoc test		SOM > PV	SOM > PV	SOM > PV	PV > SOM
(Tukey test, $P < 0.05$)		SOM > αAc2	SOM-BSNP > SOM-RS	αAc2 > PV	PV > αAc2
			SOM-BSNP > αAc2		αAc2 > SOM

Note: Data are mean ± SD. *N*, number of cells. PV, parvalbumin; SOM, somatostatin; αAc2, α-actinin-2.
[a]Depolarizing current pulse of 0.5 s to induce spikes.
[b]4 in layer II/III and 2 in layer V.

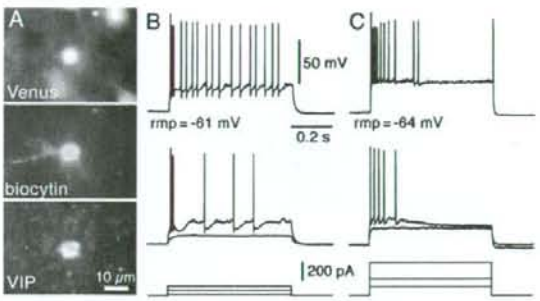

Figure 6. Venus-expressing VIP cells in layer II/III. (*A*) Immunohistochemical identification of recorded Venus-positive cells labeled by biocytin and showing VIP immunofluorescence. (*B*) A VIP cell showed the initial short-duration depolarizing hump with several spikes on it, followed by spike firing with irregular intervals. (*C*) Another VIP cell showed strong adaptation of spike firing in response to depolarizing current pulses and also irregular spike intervals.

allowed us to record nonpyramidal cells in an unbiased way irrespective of the soma size and shape.

Although the distribution of somatic size in FS cells was continuous from smaller to larger neurons (Fig. 7*B*), we looked for correlation between physiological properties and somatic size in 15 FS cells whose somata were stained with biocytin (maximum of the cross-sectional somatic area: 214 ± 65 μm^2; range, 128–311 μm^2). We did not find distinct differences in firing patterns between smaller and larger FS cells, but there was a weak correlation between input resistance and somatic size (c.c. = 0.32, $P = 0.25$; 103 ± 44 MΩ in 5 smaller cells and 69 ± 6 MΩ in 5 larger cells). The morphology of dendritic arborizations was investigated in FS basket cells whose dendrites and axons were sufficiently stained. The somatic size of FS cells correlated with the maximum vertical elongation of dendrites (c.c. = 0.55) (Fig. 7*A*), but not with the maximum horizontal distance (c.c. = 0.12) (Fig. 7*C*). Lager FS cells extended dendrites more widely in a vertical direction. Maximum vertical dendritic elongation was independent of somatic depth within layer V (c.c. = 0.06). This suggests that chemically and physiologically homogeneous FS cells are heterogeneous in their dendritic vertical dimensions, but have relatively uniform horizontal (columnar) dendritic dimensions (Fig. 7*C*). Findings were similar when observations were repeated in wild-type rats, as shown in the Appendix (Fig. 10). These data suggest that individual nonpyramidal cell subtypes, defined by combination of the spike firing, chemical expression, and axonal arborization patterns, show type-specific horizontal dendritic extensions.

Discussion

By applying BAC technology to rats, we generated, for the first time, transgenic rats with selective Venus fluorescence in GABAergic neurons. In certain brain areas, non-GABAergic neurons were labeled with Venus, but these areas were rarely overlapping in our 2 transgenic lines. Thus, at least one transgenic line can be used for selective identification of GABA cells in most areas of the forebrain. In the neocortex, we utilized the selective expression of Venus in GABAergic neurons to dissociate cortical interneurons into subtypes based on their chemical, physiological, and morphological characteristics. This is the first time that quantitative assessment of cortical interneurons using the above 6 chemical markers has been applied simultaneously to the full GABAergic cell population in the neocortex.

Selective Fluorescence Labeling of Forebrain GABA Cells in BAC Transgenic Rats

The biosynthetic enzyme for GABA, GAD, has 2 isoforms, GAD65 and GAD67. In transgenic mice produced using one of the 2 GAD promoters, only subpopulations of GABAergic cells are labeled with GFP (Oliva et al. 2000; Chattopadhyaya et al. 2004; Lopez-Bendito et al. 2004; Ma et al. 2006; Xu et al. 2006). In GAD67-GFP knock-in mice, most GABA cells are fluorescently labeled, but cells expressing only GAD65 may not be labeled. Furthermore, in GAD67-GFP knock-in mice, the GABA content is decreased because of the deletion of one GAD67 allele (Tamamaki et al. 2003). This reduction of GABA content may affect circuit formation, especially during development (Hensch 2005). Because the gene length of VGAT (~5 kb) is much shorter than those of GAD67 (~45 kb) and GAD65 (~80 kb) (Yanagawa et al. 1997; Makinae et al. 2000; Ebihara et al. 2003), we were able to construct a BAC clone containing the entire structure of VGAT, including regulatory sequences near the gene itself, to selectively label GABAergic neurons in rats. GABAergic neurons are widespread in the mammalian CNS, whereas glycinergic neurons are largely restricted to the spinal cord and brainstem (Esclapez et al. 1994; Legendre 2001). VGAT is the vesicular transporter not only for GABA but also for glycine (Sagne et al. 1997; Chaudhry et al. 1998). Therefore, it remains to be investigated whether both GABAergic and glycinergic cells are labeled with Venus in the spinal cord and brainstem.

We found Venus expression in non-GABAergic cells in a few regions, such as the relay nuclei of the thalamus in VGAT-Venus-A rats and the CA1 region of the hippocampus in VGAT-Venus-B rats. Even in these regions, however, the other line showed correct expression of Venus. Therefore, one of these 2 lines

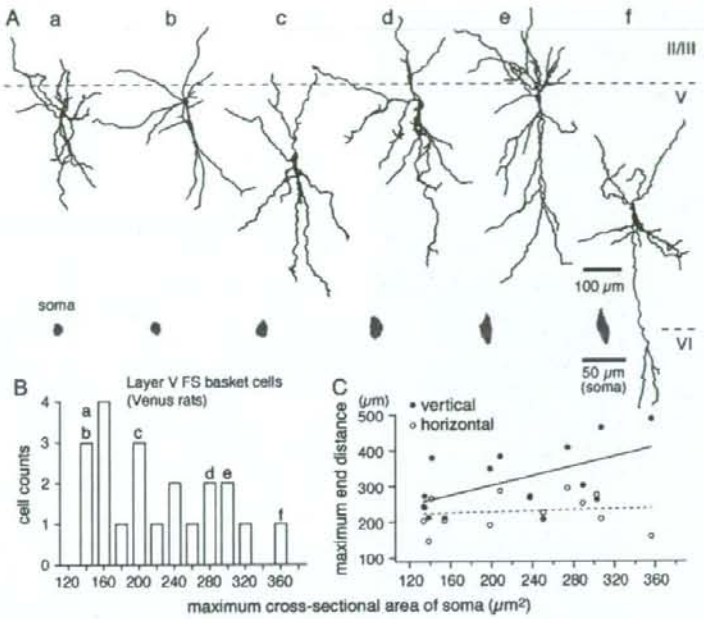

Figure 7. Large variability in the somatic size of layer V FS basket cells recorded from VGAT-Venus rats. (*A*) Dendritic reconstructions of 6 FS basket cells (a–f) in layer V sorted (left to right) according to increasing somatic cross-sectional area. Insets, somatic shapes. (*B*) Distribution of somatic cross-sectional areas. Each letter corresponds to the reconstructed cell shown in (*A*). (*C*) Relationship of dendritic arbors to the somatic cross-sectional areas. Horizontal and vertical maximum dendritic distances are calculated as the distances from somatic origin to the tip of the longest dendrite in horizontal and vertical directions, respectively. The vertical, but not horizontal, maximum distance was correlated with somatic size.

should be selected according to the investigated nucleus, region, or layer.

In the neocortex there were also subtle differences in Venus expression between the 2 lines. In VGAT-Venus-A rats, almost all GABAergic cells expressed Venus, but some layer VI pyramidal cells were weakly labeled in nonfrontal cortical areas. In VGAT-Venus-B rats, Venus fluorescence was not observed in layer VI pyramidal cells, and there was also failure to label all GABAergic cells. Nonfluorescent GABA cells in the B line belonged to subpopulations of VIP, CCK, calretinin, or α-actinin-2 expressing cells. Parvalbumin- and somatostatin-positive cells were always positive for Venus. The differential expression of Venus among GABAergic subtypes in the B line may reflect differences in the developmental origins of GABAergic neurons. Parvalbumin- and somatostatin-positive cells originate within the medial ganglionic eminence, whereas calretinin-positive cells derive from the caudal ganglionic eminence (Xu et al. 2004). The site of generation within the ganglionic eminence and its timing are critical for interneuron subtype differentiation (Butt et al. 2005). Aberrant Venus expression in some non-GABAergic cells, and the lack of Venus in specific subpopulations of GABAergic cells, may result from a positional effect, in which transcriptional regulation of the transgene is influenced by the chromosomal sequences flanking the point of transgene integration (Bessis et al. 1995).

Cortical GABA Cell Type Organization

Most GABAergic cell types identified so far can be classified based on their differential expression of a few calcium-binding proteins and neuropeptides, although individual expression patterns often include multiple morphological subtypes. LS neurogliaform cells, however, have not yet been chemically characterized. In the hippocampus, the actin-binding protein, α-actinin-2, is expressed not only in the dendrites of pyramidal cells, but also in the somata of some interneurons (Wyszynski et al. 1998; Ratzliff and Soltesz 2001), including neurogliaform cells (Price et al. 2005). Using VGAT-Venus-A rats, we found that α-actinin-2 is expressed in a subpopulation of GABAergic cells of the frontal cortex that includes LS neurogliaform cells in both layers II/III and V. α-Actinin-2 LS neurogliaform cells had an intermediate current threshold for spike induction that fell between the values for parvalbumin-expressing FS and somatostatin-positive cells. The slope of firing frequency against the injected current was less sharp in α-actinin-2 LS neurogliaform cells than in parvalbumin and somatostatin cells, and LS cells fired action potentials at relatively constant intervals, similar to FS cells, but at a much lower frequency. GABAergic nonpyramidal cells could generally be divided into basket and nonbasket cells based on their innervation preference for somatic domains. Innervation patterns of α-actinin-2–expressing LS neurogliaform cells, however, were more variable in their tendency to choose somatic targets (Figs 5*G* and 9). These physiological, chemical, and morphological characteristics suggest that cortical neurogliaform cells are a functionally distinct subgroup of cortical GABAergic cells (Tamás et al. 2003; Price et al. 2005).

The functional diversity of cortical GABAergic interneurons in the cortex remains to be investigated (Nelson 2002; Yuste 2005). Because several chemical markers are differentially

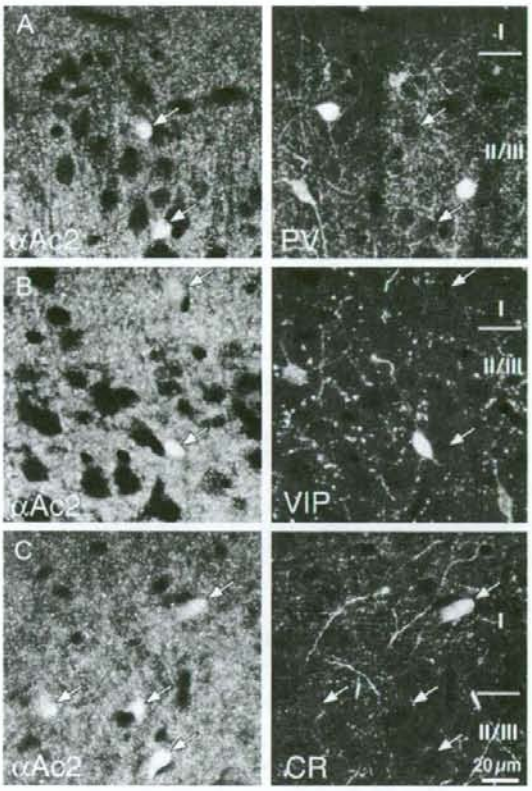

Figure 8. In the cortex, α-actinin-2–positive (αAc2) cells were separate from parvalbumin (PV) and VIP populations, but partially overlapped with calretinin cells. (*A*) Dual photomicrographs from the same microscopic field, showing the relationship of α-actinin-2– and parvalbumin-positive cells in wild-type rats. (*B*) Relationship of α-actinin-2 and VIP cells. (*C*) Relationship of α-actinin-2 and calretinin cells. Some α-actinin-2–positive cells showed calretinin immunofluorescence. Roman numerals correspond to cortical layers.

expressed in the somata of cortical GABAergic cells in a manner dependent on their developmental origin (Butt et al. 2005), it is important to know the proportion of all GABAergic neurons that can be identified from these markers. Our data demonstrate that α-actinin-2 is a chemical marker for neocortical LS neurogliaform cells, as has previously been shown for LS cells in the hippocampus (Price et al. 2005), and therefore allow the use of colocalization of 6 distinct chemical markers with Venus to estimate the proportion of GABA cells expressing at least one chemical marker (parvalbumin, somatostatin, CCK, VIP, calretinin, and α-actinin-2). We found that these 6 chemical markers cover the vast majority of GABAergic cells. Basket cells have been classified into several subtypes based on their differential expression of parvalbumin, VIP, CCK, or calretinin. Parvalbumin and CCK immunoreactivities are expressed in GABAergic cells with larger somata. Large CCK basket cells have been previously investigated in layer II/III where they are identifiable by their larger size relative to layer II/III pyramidal cells (Kawaguchi and Kubota 1998). Parvalbumin cells tend to be larger in deeper layers (Kubota et al. 1994), where they can sometimes be mistaken for layer V/VI pyramidal cells. In VGAT-Venus rats we

Table 5
Expression of the other chemical markers in α-actinin-2 cells of frontal cortex

Layer	PV	SOM	CR	VIP	CCK	CB
I	0% (75)	0% (74)	14.8% (81)	1.4% (74)	0% (78)	0% (33)
II/III	0% (81)	0% (101)	3.0% (101)	1.2% (82)	0% (97)	0% (48)
V	0% (17)	0% (20)	18.8% (16)	0% (19)	0% (14)	0% (12)
VI	0% (41)	0% (49)	16.2% (37)	0% (53)	2.4% (42)	0% (34)
Total	0% (214)	0% (244)	10.2% (235)	0.9% (228)	0.4% (231)	0% (127)

Note: Cells positive for a chemical marker/α-actinin-2 cells. PV, parvalbumin; SOM, somatostatin; CR, calretinin; CB, calbindin. Data are combined from 3 animals. ( ), number of cells positive for α-actinin-2 (denominator).

found large FS basket cells that were of similar size or shape to pyramidal cells, as well as much smaller neurons, and their vertical dendritic extent varied with somatic size. These data indicate basket cells having similar chemical and physiological characteristics can be further differentiated based on dendritic domains, even within the same layer. Because of the robust Venus fluorescence in our VGAT-Venus animals, we can now identify and record from neocortical nonpyramidal cells in an unbiased manner, irrespective of somatic size or shape.

Utility of VGAT-Venus Transgenic Rats

Largely as a result of technical advances such as gene targeting (knockout and knock-in) technology in ES cells, the mouse will continue to be a convenient mammalian model, especially for genetic and developmental studies. In contrast, the rat has for many years provided the most appropriate physiological and neurobiological model. The rat is useful for a whole range of physiological, surgical, and neurobiological manipulations that would be much more difficult in the mouse because of its smaller size (Phang 1993). Examples of such manipulations include the measurement of blood pressure, multiple automated blood sampling, and the introduction of probes into specific areas of the brain for electrophysiological recordings, cellular ablation, and drug delivery. In addition, the rat has been the preferred model for behavioral studies because rats are superior to mice in learning and generally less aggressive during handling. Furthermore, it should be possible to record Venus-positive cortical cells by direct visual guidance of 2-photon microscopy (Margrie et al. 2003). Given that cortical GABAergic neurons play a central role in generating appropriate behavioral output (Fuchs et al. 2007), VGAT-Venus rats will be an important tool for in vivo recording from cortical GABAergic neurons together with single cell fluorescence imaging.

In conclusion, the BAC technology described here permits specific fluorescent labeling of GABAergic neurons in the intact brain. This suggests possible genetic manipulation of GABAergic interneurons in the rat by driving Cre recombinase expression using the VGAT BAC construct. We expect VGAT-Venus transgenic rats to be highly useful for a multitude of in vitro or in vivo investigations of the structure and function of GABAergic neurons, both in basic research and in clinically oriented studies.

Appendix

We also investigated the following 3 characteristics in nonpyramidal cells of wild-type Wistar rats: 1) the colocalization pattern of α-actinin-2 with the other chemical markers at the somata to calculate the proportion of GABAergic cells expressing the chemical markers in VGAT-Venus rats; 2) the proportion of boutons from the nonpyramidal cells making somatic appositions in order to confirm the similarity of the somatic innervation patterns between the VGAT-Venus and wild-type

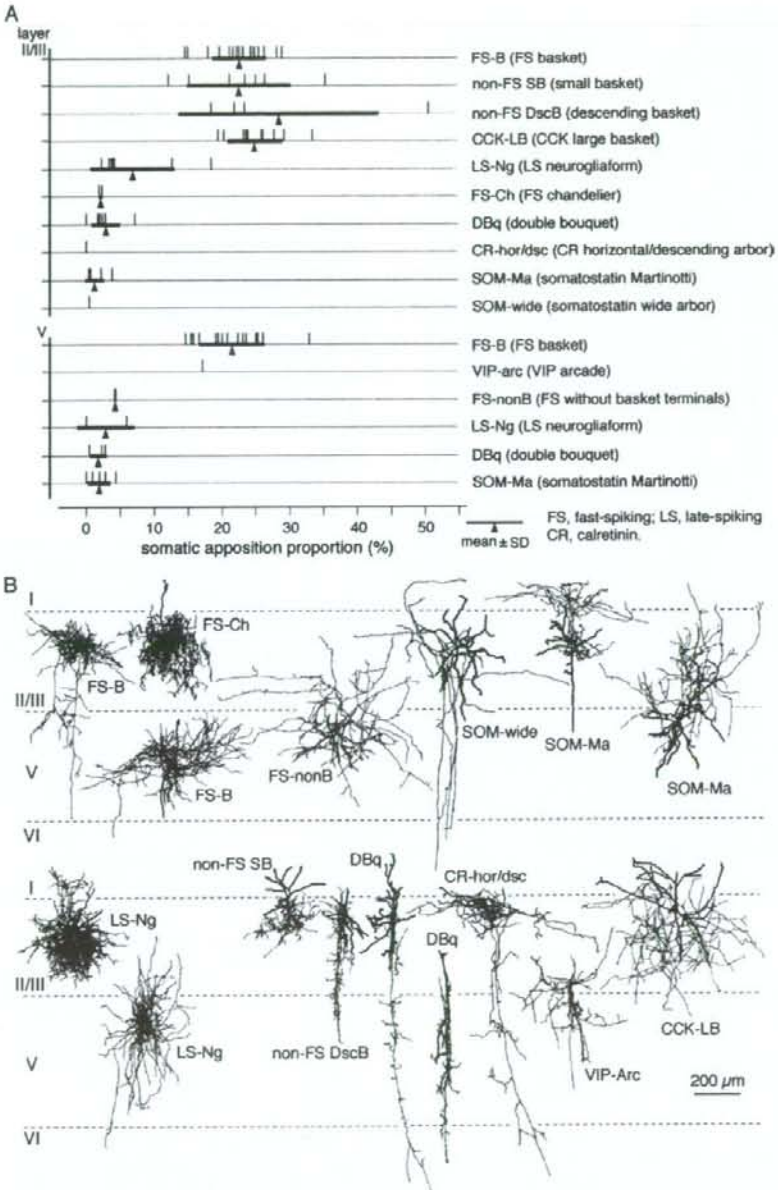

Figure 9. Somatic innervation patterns in wild-type rats. (*A*) Comparisons of the proportion of axonal boutons making appositions on other somata between nonpyramidal cell subtypes in wild-type rats. Basket and nonbasket classes were mostly differentiated. (*B*) Reconstructions of nonpyramidal cell subtypes. Somata and dendrites are shown in black, and axons in red. Ten subtypes were investigated in layer II/III: 18 FS basket cells, 2 FS chandelier cells, 7 LS neurogliaform cells, 6 somatostatin Martinotti cells, a somatostatin wide arbor cell, 11 CCK large basket cells, 7 small basket cells positive for VIP, CCK, or CRF, 4 descending basket cells positive for VIP or CRF, 7 double bouquet cells positive for VIP, CRF, or calretinin, and 1 calretinin horizontal/descending arbor cell. In layer V, 6 subtypes were investigated: 16 FS basket cells, 2 FS cells without basket terminals, 2 LS neurogliaform cells, 5 somatostatin Martinotti cells, 3 double bouquet cells positive for VIP, and a VIP arcade cell.

rats; and 3) the horizontal spread of dendrites, which, from the data of FS basket cells obtained from the VGAT-Venus rat appeared specific for each subtype.

To determine the frequency for colocalization of α-actinin-2 with the other chemical markers, we investigated the relationship of their immunofluorescences in the frontal cortex (Fig. 8). Parvalbumin-positive and somatostatin-positive cells did not express α-actinin-2, and only a very few VIP-positive and CCK-positive neurons were positive for α-actinin-2 (Table 5). However, some α-actinin-2-positive cells showed calretinin immunoreactivity, especially in layer I (14.8%),

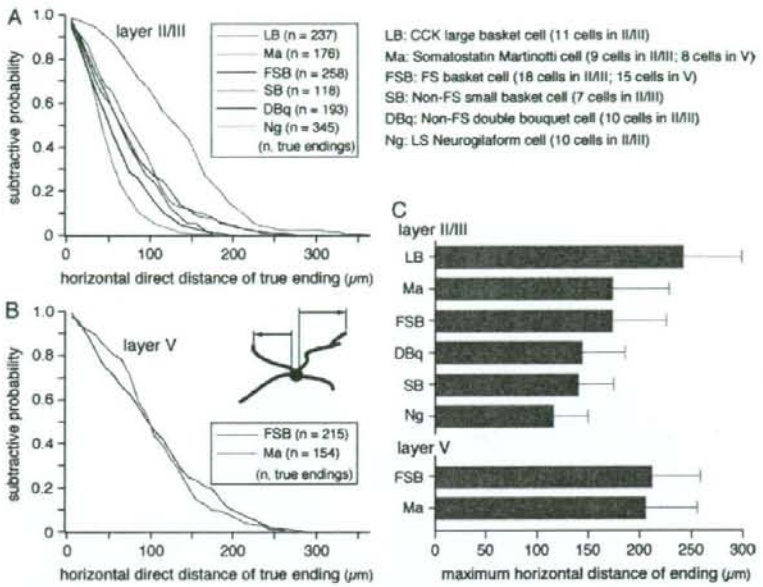

Figure 10. Dendritic horizontal extension of nonpyramidal cell subtypes. (*A*, *B*) Distributions of horizontal direct distances of true endings, measured from their somatic origins, in layers II/III and V, respectively. In layer II/III CCK large basket cells were wider than the other types ($P < 0.01$). The LS neurogliaform cells were narrower than the other types ($P < 0.01$). Double bouquet cells were narrower than CCK large basket, somatostatin Martinotti, and FS basket cells ($P < 0.01$). (*C*) Maximum horizontal dendritic spread of individual nonpyramidal cells. In layer II/III, CCK large basket cells had larger maximum dendritic spreads than did LS neurogliaform, non-FS small basket, double bouquet, and FS basket cells ($P < 0.01$), and somatostatin Martinotti cells ($P < 0.05$). FS basket cells had larger dendritic spreads than LS neurogliaform cells ($P < 0.05$).

layer V (18.8%), and layer VI (16.2%) (Table 5). Another calcium-binding protein, calbindin was not found in α-actinin-2 cells.

We compared the proportion of boutons apposed with target somata for 12 subtypes of nonpyramidal cells in wild-type rats, including previously recorded and stained cells by Karube et al. (2004), and also newly reconstructed cells (Fig. 9; 64 cells of 10 subtypes in layer II/III and 29 cells of 6 subtypes in layer V). These measurements suggest that, whereas nonpyramidal cell subtypes are different in their preferences for axonal innervation of somata, more than half of GABAergic boutons contact domains other than somata, even in basket cells. The somatic apposition proportions of LS neurogliaform cells were found to be more variable in wild-type rats.

We compared the horizontal spread of dendrites among the 6 GABAergic cell subtypes previously described by Kawaguchi et al. (2006) (Fig. 10). The mean horizontal length of dendrites (as measured from soma to uncut endings) of the layer V FS basket cell was 117 ± 68 μm (249 true endings from 14 cells) in Venus rats, and 109 ± 66 μm (215 from 15 cells) in tissue from wild-type rats (Fig. 10*B*). Horizontal dendritic distances of layer V somatostatin Martinotti cells were similar, being 109 ± 55 μm (154 from 8 cells). In layer II/III, dendrites of CCK large basket cells had a longer horizontal reach than dendrites in LS neurogliaform, double bouquet, non-FS small basket, FS basket, and somatostatin Martinotti cells ($P < 0.01$; Fig. 10*A*). LS neurogliaform cells were also narrower than all other types ($P < 0.01$), and double bouquet cells were narrower than the CCK large basket, somatostatin Martinotti, and FS basket cells ($P < 0.01$). Next, the maximum horizontal distance (horizontal spread) was obtained from individual cells. The maximum horizontal dendritic spread in layer V FS basket cells was 230 ± 47 μm (14 cells) from Venus rats and 212 ± 47 μm (15 cells) from wild-type rats (Fig. 10*C*). That of layer V somatostatin Martinotti cells was similar (206 ± 50 μm, 8 cells). In layer II/III, CCK large basket cells had larger maximum horizontal spread than LS neurogliaform, non-FS small basket, double bouquet, and FS basket cells ($P < 0.01$; Fig. 10*C*).

These observations from wild-type rats, combined with those from VGAT-Venus rats, support the normal differentiation of cortical GABAergic cells in VGAT-Venus rats, and demonstrate that α-actinin-2 is a useful chemical marker for a distinct cortical interneuron subtype. Further, they suggest a cortical interneurons maintain an inherent, cell type-specific horizontal dendritic territory.

Notes

The authors thank Ms M. Saito and Mr Y. Ito for technical assistances, and Drs A. Gulledge, Y. Kubota and M. Morishima for discussion and comments. We also thank staffs in Center for Experimental Animals, National Institute for Physiological Sciences (NIPS). We are grateful to Dr A. Miyawaki for providing pCS2-Venus, to Dr M. D. Lalioti for pKOV-Kan and pDF25 plasmids, to Dr A.H. Beggs for an antiserum against α-actinin-2, and to Dr N. Tamamaki for a rabbit antiserum against eGFP. We are also grateful to Dr T. Kosaka for helpful discussions about Venus expression patterns. This work was supported by Grant-in-Aids for Scientific Research from the Ministry of Education, Culture, Sports, Science and Technology (MEXT) and on Psychiatric and Neurological Diseases and Mental Health from the Ministry of Health, Labor and Welfare of Japan, and also supported by The Uehara Memorial Foundation and Brain Science Foundation. This paper is dedicated to the late Ms Kazuko Kawaguchi who had supported Y.K. continuously.
Conflict of Interest: None declared.

Address correspondence to Yasuo Kawaguchi, Division of Cerebral Circuitry, National Institute for Physiological Sciences, Myodaiji, Okazaki 444-8585, Japan. Email: yasuo@nips.ac.jp, or to Yuchio Yanagawa, Department of Genetic and Behavioral Neuroscience, Gunma University Graduate School of Medicine, Maebashi 371-8511, Japan. Email: yanagawa@med.gunma-u.ac.jp.

References

Bessis A, Salmon AM, Zoli M, Le Novere N, Picciotto M, Changeux JP. 1995. Promoter elements conferring neuron-specific expression of the beta 2-subunit of the neuronal nicotinic acetylcholine receptor studied in vitro and in transgenic mice. Neuroscience. 69: 807-819.

Butt SJ, Fuccillo M, Nery S, Noctor S, Kriegstein A, Corbin JG, Fishell G. 2005. The temporal and spatial origins of cortical interneurons predict their physiological subtype. Neuron. 48:591–604.

Cauli B, Porter JT, Tsuzuki K, Lambolez B, Rossier J, Quenet B, Audinat E. 2000. Classification of fusiform neocortical interneurons based on unsupervised clustering. Proc Natl Acad Sci USA. 97:6144–6149.

Chattopadhyaya B, Di Cristo G, Higashiyama H, Knott GW, Kuhlman SJ, Welker E, Huang ZJ. 2004. Experience and activity-dependent maturation of perisomatic GABAergic innervation in primary visual cortex during a postnatal critical period. J Neurosci. 24: 9598–9611.

Chaudhry FA, Reimer RJ, Bellocchio EE, Danbolt NC, Osen KK, Edwards RH, Storm-Mathisen J. 1998. The vesicular GABA transporter, VGAT, localizes to synaptic vesicles in sets of glycinergic as well as GABAergic neurons. J Neurosci. 18:9733–9750.

DeFelipe J, Hendry SH, Jones EG. 1986. A correlative electron microscopic study of basket cells and large GABAergic neurons in the monkey sensory-motor cortex. Neuroscience. 17:991–1009.

Ebihara S, Obata K, Yanagawa Y. 2003. Mouse vesicular GABA transporter gene: genomic organization, transcriptional regulation and chromosomal localization. Brain Res Mol Brain Res. 110:126–139.

Esclapez M, Tillakaratne NJ, Kaufman DL, Tobin AJ, Houser CR. 1994. Comparative localization of 2 forms of glutamic acid decarboxylase and their mRNAs in rat brain supports the concept of functional differences between the forms. J Neurosci. 14:1834–1855.

Ferezou I, Cauli B, Hill EL, Rossier J, Hamel E, Lambolez B. 2002. 5-HT_3 receptors mediate serotonergic fast synaptic excitation of neocortical vasoactive intestinal peptide/cholecystokinin interneurons. J Neurosci. 22:7389–7397.

Fuchs EC, Zivkovic AR, Cunningham MO, Middleton S, LeBeau FEN, Bannerman DM, Rozov A, Whittington MA, Traub RD, Rawlins JNP, et al. 2007. Recruitment of parvalbumin-positive interneurons determines hippocampal function and associated behavior. Neuron. 53:591–604.

Gonchar Y, Burkhalter A. 1997. Three distinct families of GABAergic neurons in rat visual cortex. Cereb Cortex. 7:347–358.

Gulledge AT, Park SB, Kawaguchi Y, Stuart GJ. 2007. Heterogeneity of phasic cholinergic signalling in neocortical neurons. J Neurophysiol. 97:2215–2229.

Gupta A, Wang Y, Markram H. 2000. Organizing principles for a diversity of GABAergic interneurons and synapses in the neocortex. Science. 287:273–278.

Heintz N. 2001. BAC to the future: the use of BAC transgenic mice for neuroscience research. Nat Rev Neurosci. 2: 861–870.

Hensch TK. 2005. Critical period plasticity in local cortical circuits. Nat Rev Neurosci 6:877–888.

Jones EG. 1975. Varieties and distribution of non-pyramidal cells in the somatic sensory cortex of the squirrel monkey. J Comp Neurol. 160:205–267.

Karube F, Kubota Y, Kawaguchi Y. 2004. Axon branching and synaptic bouton phenotypes in GABAergic nonpyramidal cell subtypes. J Neurosci. 24:2853–2865.

Kawaguchi Y. 1997. Selective cholinergic modulation of cortical GABAergic cell subtypes. J Neurophysiol. 78:1743–1747.

Kawaguchi Y, Karube F, Kubota Y. 2006. Dendritic branch typing and spine expression patterns in cortical nonpyramidal cells. Cereb Cortex. 16:696–711.

Kawaguchi Y, Kondo S. 2002. Parvalbumin, somatostatin and cholecystokinin as chemical markers for specific GABAergic interneuron types in the rat frontal cortex. J Neurocytol. 31:277–287.

Kawaguchi Y, Kubota Y. 1993. Correlation of physiological subgroupings of nonpyramidal cells with parvalbumin- and calbindin$_{D28k}$-immunoreactive neurons in layer V of rat frontal cortex. J Neurophysiol. 70:387–396.

Kawaguchi Y, Kubota Y. 1996. Physiological and morphological identification of somatostatin- or vasoactive intestinal polypeptide-containing cells among GABAergic cell subtypes in rat frontal cortex. J Neurosci. 16:2701–2715.

Kawaguchi Y, Kubota Y. 1997. GABAergic cell subtypes and their synaptic connections in rat frontal cortex. Cereb Cortex. 7: 476–486.

Kawaguchi Y, Kubota Y. 1998. Neurochemical features and synaptic connections of large physiologically-identified GABAergic cells in the rat frontal cortex. Neuroscience. 85:677–701.

Kubota Y, Hatada S, Kondo S, Karube F, Kawaguchi Y. 2007. Neocortical inhibitory terminals innervate dendritic spines targeted by thalamocortical afferents. J Neurosci. 27:1139–1150.

Kubota Y, Hattori R, Yui Y. 1994. Three distinct subpopulations of GABAergic neurons in rat frontal agranular cortex. Brain Res. 649:159–173.

Kubota Y, Kawaguchi Y. 1997. Two distinct subgroups of cholecystokinin-immunoreactive cortical interneurons. Brain Res. 752:175–183.

Lalioti M, Heath J. 2001. A new method for generating point mutations in bacterial artificial chromosomes by homologous recombination in Escherichia coli. Nucleic Acids Res. 29:E14.

Legendre P. 2001. The glycinergic inhibitory synapse. Cell Mol Life Sci. 58:760–793.

Lopez-Bendito G, Sturgess K, Erdelyi F, Szabo G, Molnar Z, Paulsen O. 2004. Preferential origin and layer destination of GAD65-GFP cortical interneurons. Cereb Cortex. 14:1122–1133.

Ma Y, Hu H, Berrebi AS, Mathers PH, Agmon A. 2006. Distinct subtypes of somatostatin-containing neocortical interneurons revealed in transgenic mice. J Neurosci. 26:5069–5082.

Makinae K, Kobayashi T, Kobayashi T, Shinkawa H, Sakagami H, Kondo H, Tashiro F, Miyazaki J, Obata K, Tamura S, et al. 2000. Structure of the mouse glutamate decarboxylase 65 gene and its promoter: preferential expression of its promoter in the GABAergic neurons of transgenic mice. J Neurochem. 75:1429–1437.

Margrie TW, Meyer AH, Caputi A, Monyer H, Hasan MT, Schaefer AT, Denk W, Brecht M. 2003. Targeted whole-cell recordings in the mammalian brain in vivo. Neuron. 39:911–918.

Marin-Padilla M. 1969. Origin of the pericellular baskets of the pyramidal cells of the human motor cortex: a Golgi study. Brain Res. 14:633–646.

Markram H, Toledo-Rodriguez M, Wang Y, Gupta A, Silberberg G, Wu C. 2004. Interneurons of the neocortical inhibitory system. Nat Rev Neurosci. 5:793–807.

Melchitzky DS, Eggan SM, Lewis DA. 2005. Synaptic targets of calretinin-containing axon terminals in macaque monkey prefrontal cortex. Neuroscience. 130:185–195.

Meyer AH, Katona I, Blatow M, Rozov A, Monyer H. 2002. In vivo labeling of parvalbumin-positive interneurons and analysis of electrical coupling in identified neurons. J Neurosci. 22:7055–7064.

Morishima M, Kawaguchi Y. 2006. Recurrent connection patterns of corticostriatal pyramidal cells in frontal cortex. J Neurosci. 26:4394–4405.

Nagai T, Ibata K, Park ES, Kubota M, Mikoshiba K, Miyawaki A. 2002. A variant of yellow fluorescent protein with fast and efficient maturation for cell-biological applications. Nat Biotechnol. 20: 87–90.

Nelson S. 2002. Cortical microcircuits: diverse or canonical? Neuron. 36:19–27.

Oliva AA, Jr., Jiang M, Lam T, Smith KL, Swann JW. 2000. Novel hippocampal interneuronal subtypes identified using transgenic mice that express green fluorescent protein in GABAergic interneurons. J Neurosci. 20:3354–3368.

Phang C-H. 1993. Introduction to the physiology and husbandry of the rat. In: Murphy D, Carter DA, editors. Methods in molecular biology: transgenesis techniques. Totowa, NJ: Humana Press. p. 247–251.

Porter JT, Cauli B, Tsuzuki K, Lambolez B, Rossier J, Audinat E. 1999. Selective excitation of subtypes of neocortical interneurons by nicotinic receptors. J Neurosci. 19:5228–5235.

Price CJ, Cauli B, Kovacs ER, Kulik A, Lambolez B, Shigemoto R, Capogna M. 2005. Neurogliaform neurons form a novel inhibitory network in the hippocampal CA1 area. J Neurosci. 25:6775–6786.

Ratzliff AD, Soltesz I. 2001. Differential immunoreactivity for alpha-actinin-2, an N-methyl-D-aspartate-receptor/actin binding protein, in hippocampal interneurons. Neuroscience. 103:337–349.

Sagne C, El Mestikawy S, Isambert MF, Hamon M, Henry JP, Giros B, Gasnier B. 1997. Cloning of a functional vesicular GABA and glycine transporter by screening of genome databases. FEBS Lett. 417:177–183.

Somogyi P, Klausberger T. 2005. Defined types of cortical interneurone structure space and spike timing in the hippocampus. J Physiol. 562:9–26.

Somogyi P, Tamás G, Lujan R, Buhl EH. 1998. Salient features of synaptic organisation in the cerebral cortex. Brain Res Brain Res Rev. 26:113–135.

Sugino K, Hempel CM, Miller MN, Hattox AM, Shapiro P, Wu C, Huang ZJ, Nelson SB. 2006. Molecular taxonomy of major neuronal classes in the adult mouse forebrain. Nat Neurosci. 9:99–107.

Takahashi R, Hirabayashi M, Ueda M. 1999. Production of transgenic rats using cryopreserved pronuclear-stage zygotes. Transgenic Res. 8:397–400.

Tamamaki N, Yanagawa Y, Tomioka R, Miyazaki J, Obata K, Kaneko T. 2003. Green fluorescent protein expression and colocalization with calretinin, parvalbumin, and somatostatin in the GAD67-GFP knock-in mouse. J Comp Neurol. 467:60–79.

Tamás G, Lörincz A, Simon A, Szabadics J. 2003. Identified sources and targets of slow inhibition in the neocortex. Science. 299: 1902–1905.

Toledo-Rodriguez M, Blumenfeld B, Wu C, Luo J, Attali B, Goodman P, Markram H. 2004. Correlation maps allow neuronal electrical properties to be predicted from single-cell gene expression profiles in rat neocortex. Cereb Cortex. 14:1310–1327.

Wang Y, Gupta A, Toledo-Rodriguez M, Wu CZ, Markram H. 2002. Anatomical, physiological, molecular and circuit properties of nest basket cells in the developing somatosensory cortex. Cereb Cortex. 12:395–410.

Wyszynski M, Kharazia V, Shanghvi R, Rao A, Beggs AH, Craig AM, Weinberg R, Sheng M. 1998. Differential regional expression and ultrastructural localization of alpha-actinin-2, a putative NMDA receptor-anchoring protein, in rat brain. J Neurosci. 18:1383–1392.

Xu Q, Cobos I, De La Cruz E, Rubenstein JL, Anderson SA. 2004. Origins of cortical interneuron subtypes. J Neurosci. 24:2612–2622

Xu X, Roby KD, Callaway EM. 2006. Mouse cortical inhibitory neuron type that coexpresses somatostatin and calretinin. J Comp Neurol. 499:144–160.

Yanagawa Y, Kobayashi T, Kamei T, Ishii K, Nishijima M, Takaku A, Tamura S. 1997. Structure and alternative promoters of the mouse glutamic acid decarboxylase 67 gene. Biochem J. 326:573–578.

Yuste R. 2005. Origin and classification of neocortical interneurons. Neuron. 48:524–527.